IEEE Access
Multidisciplinary ⋮ Rapid Review ⋮ Open Access Journal

Received 29 April 2024, accepted 11 July 2024, date of publication 18 July 2024, date of current version 31 July 2024.

Digital Object Identifier 10.1109/ACCESS.2024.3430323

RESEARCH ARTICLE

B-Spline Artificial Neural Networks in Robust Induction Motor Control

FRANCISCO BELTRAN-CARBAJAL[1], HUGO YAÑEZ-BADILLO[2], DANIEL GALVAN-PEREZ[3], IVAN RIVAS-CAMBERO[3], (Member, IEEE), DAVID SOTELO[4], AND CARLOS SOTELO[4]

[1]Departamento de Energía, Universidad Autónoma Metropolitana–Unidad Azcapotzalco, Mexico City 02200, Mexico
[2]Departamento de Investigación, Tecnológico de Estudios Superiores de Tianguistenco (TecNM), Santiago Tianguistenco 52650, Mexico
[3]Departamento de Posgrado, Universidad Politécnica de Tulancingo, Tulancingo 43629, Mexico
[4]Tecnológico de Monterrey, School of Engineering and Sciences, Monterrey 64849, Mexico

Corresponding author: David Sotelo (david.sotelo@tec.mx)

ABSTRACT Artificial intelligence stands for an excellent alternative to be considered in development of new adaptive high-efficiency control design methodologies for uncertain modern complex engineering systems driven by electric motors. In this sense, artificial neural networks can be embedded within innovative nonlinear control design strategies to add capabilities to neutralize various kinds of dynamic perturbations or uncertainties that can significantly deteriorate the operating efficiency of nonlinear electric motor systems. This paper introduces a novel adaptive sliding mode nonlinear control method based on B-spline artificial neural networks for efficient tracking of optimal smooth operating reference trajectories in induction or asynchronous motors under substantially disturbed operational scenarios. Robustness regarding nonlinear theoretical mathematical modelling errors, parametric uncertainty and unknown external multiple-frequency oscillating disturbing influences is considered. Numerical experiments involving multiple disturbed operating case studies are presented to demonstrate the effective performance of the proposed robust adaptive artificial neural-network control scheme on large horsepower three-phase induction motors. Finally, a comparative evaluation is conducted, emphasizing system performance through the use of index performance criteria, and comparing the proposed adaptive robust B-spline approach with a nonlinear passivity-based controller. New insights to extend the introduced adaptive neural network robust control design strategy to other considerably perturbed practical nonlinear engineering systems are thus provided.

INDEX TERMS Artificial neural networks, intelligent control, machine control systems, artificial intelligence.

I. INTRODUCTION

Artificial intelligence has permeated nearly every global industry sector, initiating a paradigm shift in approaching the most intricate problems. Defined as a computing system's ability to perform tasks typically requiring human intervention, like decision-making, pattern recognition, and autonomous learning, artificial intelligence is driving this digital revolution [1]. A broad array of tools and techniques fuel this change, including but not limited to artificial neural networks, machine learning, deep learning, fuzzy logic, expert systems, and genetic algorithms [2]. Artificial intelligence technologies have been successfully exploited to develop innovating applications in several engineering fields and important sectors such as in the food production ecosystem, agriculture, healthcare, finance, signal processing, remote sensing, forecasting, computer vision and social media [3], [4]. Artificial neural networks have been also proposed for health monitoring of rotating machinery based on information of vibration signals [5].

Moreover, many commercial technological applications of artificial intelligence for the transportation sector have been developed [6], [7]. Transportation stands for an important component in the construction of smart cities [7]. In fact, this sector is undergoing a transformation process driven by the adoption of electric vehicles. This change benefits

The associate editor coordinating the review of this manuscript and approving it for publication was Feifei Bu.

the environment and opens the door to new possibilities for improving energy efficiency and control technology, particularly in electric motor control. In this context, Artificial Intelligence (AI) offers several advantages. First, it allows for increased motor operation efficiency through real-time optimization of control parameters. This can lead to improved energy efficiency and, therefore, greater autonomy for electric vehicles [8]. Second, AI systems can adapt and learn from different operating conditions, enhancing the robustness of motor control against variations in road conditions or vehicle load [9]. Furthermore, integration of artificial intelligence in control of electric motors can facilitate the development of autonomous vehicles, as these systems can process a large amount of information and make complex control decisions in fractions of a second [10].

The implementation of neural networks in the control of motors of electric vehicles represents a great promise and a necessity in the contemporary context of electric mobility [11]. Drawing inspiration from the functioning of the human brain, these networks, within the context of artificial intelligence, empower computer systems to acquire knowledge from experience and adapt to novel situations. Its utility lies in its ability to model and control complex systems more effectively than traditional techniques [12]. For electric motors with a complicated or ill-defined mathematical model, neural networks can learn directly from sensor data without needing a precise mathematical model. This ability to learn and adapt results in more accurate and efficient control and facilitates implementation [13]. Over time, as neural networks know from the engine and driving data, they can optimize engine performance and improve energy efficiency. In addition, they bring remarkable robustness to the system, handling variations in road conditions and vehicle load and adjusting engine control accordingly [14]. This flexibility is advantageous in unforeseen or extreme conditions where conventional control models might fall short. Neural networks could play a crucial role in developing autonomous vehicles [15]. These systems require the ability to process vast amounts of information and make complex control decisions in fractions of a second, a task for which neural networks are ideally suited. Thus, artificial neural networks represent an excellent choice to develop innovating adaptive motion control technology for a wide variety of complex modern engineering systems driven by electric motors, reducing substantially dependency on detailed nonlinear mathematical models based on physics and accurate knowledge of their respective parameters.

This paper deals with the strategic integration of B-spline artificial neural networks to create a novel effective solution alternative to the robust control problem for the efficient operating motion trajectory planning tracking on uncertain three-phase induction or asynchronous motors subjected to external, vibrating or oscillating disturbances. In this regard, induction motors have been widely used as controlled motion actuators in various industrial applications of electrical, mechanical, electromechanical and mechatronic engineering systems under perturbed operating scenarios as well. Several conventional control techniques for induction motors based on nonlinear mathematical models have been described in detail in [16], [17], [18], and [19] and references therein. A wide range of industrial systems driven by electric motors can be perturbed by uncertain multiple-frequency harmful forced vibrations during their operation. Vibrations or oscillations can be induced by commonly unavoidable unbalance in conventional manufacturing processes of rotating components [20], [21]. In addition, electric motors are currently used as actuators to suppress forced vibrations affecting flexible mechanical systems [22]. Implementation of an important variety of active vibration control techniques utilizes properly controlled electric motors to generate variable electromagnetic torque to suppress damaging variable vibrations. In this sense, characteristics of dangerous vibrations adversely influencing to linear or nonlinear, oscillatory mechanical systems are first established. Next, robust vibration control torques or forces should be efficiently supplied by the employed actuators.

A new adaptive nonlinear control design approach for robust tracking of desired smooth reference profiles for both speed and rotor magnetic flux on uncertain induction motors under influence of unknown external torque vibrations is introduced in the present article. B-spline artificial neural networks and sliding mode theory are integrated in the predefined motion profile tracking control design process. In contrast to other important contributions to efficiently regulate the induction motor operation, capabilities to attenuate uncertain multiple-frequency vibrating disturbances are incorporated in the presented neural network control scheme. Moreover, active suppression of disturbances due to unmodeled dynamics, parametric uncertainty and theoretical modelling errors can be also attained. Incorporation of additional observer algorithms for real-time disturbance estimation is not required. Information of vibrating disturbances can be extracted from the neural adaptive control scheme. Numerical results of several operating studies are furthermore presented to reveal the effective performance of the proposed control scheme on large horsepower three-phase induction motors. The introduced adaptive neural network robust control design approach can be extended to develop solutions of nonlinear control problems for diverse types of electric motors.

The subsequent sections of this document are organized as follows: Section II offers a concise introduction to the hardware implementation of neural networks in microcontroller-based embedded systems, highlighting the feasibility of employing this type of controllers. Description of the mathematical model for the nonlinear induction motor system, perturbed by uncertain vibrating torque with multiple excitation frequencies is presented in section III. The problem of efficient motion planning trajectory tracking control on uncertain three-phase electric induction motor systems

under influence of completely unknown multiple-frequency external torque vibrations is addressed in Section IV. The proposed adaptive robust nonlinear control design strategy based on B-spline artificial neural networks and sliding mode theory executes an efficient tracking of the angular speed and rotor magnetic flux, where the capability of robustness with respect several classes of disturbances or uncertainties is demonstrated. In Section V numerical simulation results to successfully corroborate the planning motion tracking efficacy and robustness of the proposed neural nonlinear control design strategy are discussed. A very good active attenuation level of multi-frequency forced oscillations is evidenced. Finally, the main conclusions of the present contribution and subsequent relevant research works are finally summarized in Section VI.

II. NEURAL NETWORK IMPLEMENTATION IN MICROCONTROLLER-BASED EMBEDDED SYSTEMS

Artificial neural networks are distributed parallel processing systems comprising nonlinear elements designed to emulate the essential functions of biological neurons. These networks can be implemented using either general-purpose or specialized hardware. The practical deployment of artificial neural networks can be achieved through hardware, providing flexibility to adapt to diverse applications and computational environments emulating the distributed and highly interconnected nature of the biological nervous system, offering potential solutions to complex and varied problems across fields ranging from artificial intelligence to specific task resolution.

In the realm of automatic control, integrating sliding mode control schemes and B-Spline neural networks represents an advanced amalgamation of robustness and computational efficiency. Sliding mode controllers are renowned for their robustness and capability to manage uncertainties and disturbances, though they can be computationally demanding in complex systems. Conversely, B-Spline neural networks are noted for their computational efficiency, with complexity and runtime performance contingent on the neurons employed.

The study by [23] delves into applying B-Spline neural networks in control systems, emphasizing their effectiveness in real-time control environments. These networks can locally control their output behaviour, making them suitable for on-line estimation of system dynamics, a crucial capability in nonlinear control applications requiring adaptability and swift response to dynamic changes. B-spline neural networks are essential in estimating unknown dynamics of nonlinear systems, enabling efficient local tuning of weights and facilitating rapid learning of arbitrary nonlinear functions.

In [24], feedforward neural networks with tangent sigmoid activation functions are used for precise real-time estimation of muscle forces during cycling activities. These networks, tailored for embedded systems, balance precision and performance, considering the computational limitations of these environments. The activation function of the hidden neurons is optimized to enhance performance in embedded settings, with highlighted methods to optimize computational performance. Reference [25] addresses the real-time implementation of position control algorithms using B-Spline neural networks for voice coil motors. These networks offer faster convergence rates and lower computational loads, making them suitable for microcontrollers with limited computing capabilities. They also mitigate common control system problems like "chattering," facilitating smoother, more stable control.

Furthermore, implementing neural networks in microcontrollers, especially for real-time applications, requires balancing network performance with hardware limitations. Reference [26] addresses memory optimization in implementing binary neural networks in microcontrollers. This approach significantly reduces computational load and memory usage, which is crucial for real-time deployment in resource-limited microcontrollers.

Binary neural networks show improvements in accuracy, memory footprint, and latency, which are essential for real-time applications. Reference [27] presents a strategy for implementing multilayer perceptron neural networks in microcontrollers. Their study reveals a linear relationship between hyperparameters and processing time, suggesting suitability for real-time applications requiring neural network capabilities. Subsequently, [28] proposes a memory optimization technique for multilayer perceptron neural networks in 8-bit microcontrollers, enabling more extensive, more complex network architectures in low-cost, low-power devices.

On the other hand, [29] compared machine learning algorithms for estimating lithium-ion battery parameters, focusing on neural network implementation in STM32 microcontrollers. This study demonstrates the feasibility of efficiently implementing neural networks in microcontrollers, balancing the model size and accuracy, which is crucial for real-time applications. Additionally, in [27] and [30], it is indicated that neural network implementations in microcontrollers for real-time applications are feasible without incurring a significant computational burden. Reference [27] demonstrates the effective use of multilayer perceptron neural networks in microcontrollers, highlighting a direct correlation between neural network hyperparameters and processing time, thus enabling efficient real-time performance. Reference [30] extends this by successfully integrating more complex neural network architectures into real-time control applications. These findings underscore that with strategic design and optimization, deploying neural networks in microcontroller-based systems can be done effectively, catering to the demands of real-time operations without overwhelming the system's computational resources.

For the implementation of adaptive control using B-spline neural networks in a microcontroller, Digital Signal Processors (DSPs) can be a suitable selection, but careful consideration should be made. The choice hinges on factors such as the computational prowess to handle the real-time demands of the adaptive control algorithm, the availability of ample memory for storing neural network parameters,

and robust peripheral support for seamless interfacing with sensors and communication modules.

III. DYNAMIC MODEL OF THE INDUCTION MOTOR UNDER INFLUENCE OF MULTIPLE-FREQUENCY OSCILLATORY TORQUE

The transformed two-phase equivalent mathematical model employed to approximately describe the nonlinear dynamics into an operational window of time of the three-phase squirrel-cage induction motor considered in the present study is given by using (1), [17]. It is assumed that this multivariable nonlinear energy conversion system is balanced and symmetrical. Reasonable theoretical modelling errors, related to unpredictable disturbances impacting the nonlinear induction motor model, can be effectively addressed from a control design perspective through the use of artificial neural networks. Interested reader on derivation of mathematical models of the induction motor dynamics in several reference frames is also referred to the books [18], [19], [31].

$$\begin{aligned}\frac{d}{dt}\psi_{Ra} &= -\frac{R_R}{L_R}\psi_{Ra} - N_p\omega_R\psi_{Rb} + \frac{R_R M}{L_R}I_{Sa}\\ \frac{d}{dt}\psi_{Rb} &= -\frac{R_R}{L_R}\psi_{Rb} + N_p\omega_R\psi_{Ra} + \frac{R_R M}{L_R}I_{Sb}\\ \frac{d}{dt}\omega_R &= \frac{1}{J}\tau_e - \frac{b}{J}\omega_R - \frac{1}{J}\tau_L\end{aligned} \tag{1}$$

In the two-phase motor model representation (1), transformed magnetic fluxes in rotor are described by ψ_{Ra} and ψ_{Rb}. The phase electric currents I_{Sa} and I_{Sb} are used as control variables or signals. Stator, rotor and mutual inductance parameters are respectively denoted by L_S, L_R and M. Stator and rotor winding resistance parameters are represented by R_S and R_R. N_p stands for the number of rotor pole pairs. Equivalent parameters of the mechanical subsystem are the moment of inertia J, and the viscous damping b.

The electromagnetic torque τ_e generated by the induction motor is given by

$$\tau_e = \frac{N_p M}{L_R}\left(I_{Sb}\psi_{Ra} - I_{Sa}\psi_{Rb}\right) \tag{2}$$

which should compensate the possibly uncertain mechanical load dynamics $\tau_L(t)$ and regulate the operating angular velocity ω_R of the electric motor rotor simultaneously. Indeed, there are several architectures of electrical drive motors to electromagnetically generate control torque τ_e for the same rotational mechanical dynamics representation. Thence, the presented control design approach can be extended to other kinds of electric machines under substantially perturbed operational environments.

In the present work, it is considered that the motor rotor can be subjected to uncertain hazardous multiple-frequency oscillatory torque disturbances $\tau_L(t)$ into an operating window of time described as

$$\tau_L(t) = \overline{\tau}_0 + \sum_{j=1}^{m}\overline{\tau}_j\left(\sin\Omega_j t + \varphi_j\right) \tag{3}$$

where $\overline{\tau}_j$, Ω_j and φ_j stand for unknown amplitudes, frequencies and phases of the m harmonic constitutive torque terms. Variable parameters of vibrating torque components can be also admitted. Rotor unbalance in rotating machinery can lead to the induction of oscillatory disturbances or harmonic vibrations [32]. In electric vehicles driven by in-wheel motors, exogenous disturbances can provoke perilous vibrations as well [33]. Oscillatory torque with several excitation frequencies can be provided by the perturbed multiple-degree-of-freedom vibrating mechanical system connected to the motor rotor. Possible theoretical modelling errors, parametric uncertainty and external perturbations in mechanical system dynamics can be incorporated in the uncertain load torque for control design.

Oscillatory load torque can be generated by the perturbed uncertain multidegree-of-freedom vibratory rotational system

$$\begin{aligned}\mathbf{J}\frac{d^2}{dt^2}\boldsymbol{\theta} + \mathbf{K}\boldsymbol{\theta} &= \boldsymbol{\tau}_p\\ \tau_L &= \mathbf{P}\boldsymbol{\theta}\end{aligned} \tag{4}$$

Here $\boldsymbol{\theta} \in \mathbb{R}^m$ represents the angular displacement vector of the vibrating rotor system driven by the electric motor, and $\boldsymbol{\tau}_p \in \mathbb{R}^m$ stands for a harmonic excitation perturbation vector. Inertia and stiffness matrices are denoted respectively by $\mathbf{J}, \mathbf{K} \in \mathbb{R}^{m\times m}$, and $\mathbf{P} \in \mathbb{R}^{m\times m}$ denotes a perturbation output matrix. Multidegree-of-freedom rotor system dynamics is assumed to be uncertain in the presented artificial intelligence control design perspective. Then, the new adaptive control approach should perform desired motion planning tracking without knowledge of theoretical dynamic modelling, rotor system parameters and harmonic perturbations.

Relationships of three-phase to two-phase electric signals are given by [17] and [19]

$$\begin{bmatrix}\lambda_{Ra}\\ \lambda_{Rb}\\ \lambda_{R0}\end{bmatrix} = \sqrt{\frac{2}{3}}\begin{bmatrix}1 & -\frac{1}{2} & -\frac{1}{2}\\ 0 & \frac{\sqrt{3}}{2} & -\frac{\sqrt{3}}{2}\\ \frac{1}{\sqrt{2}} & \frac{1}{\sqrt{2}} & \frac{1}{\sqrt{2}}\end{bmatrix}\begin{bmatrix}\psi_{R1}\\ \psi_{R2}\\ \psi_{R3}\end{bmatrix} \tag{5}$$

$$\begin{bmatrix}I_{Sa}\\ I_{Sb}\\ I_{S0}\end{bmatrix} = \sqrt{\frac{2}{3}}\begin{bmatrix}1 & -\frac{1}{2} & -\frac{1}{2}\\ 0 & \frac{\sqrt{3}}{2} & -\frac{\sqrt{3}}{2}\\ \frac{1}{\sqrt{2}} & \frac{1}{\sqrt{2}} & \frac{1}{\sqrt{2}}\end{bmatrix}\begin{bmatrix}I_{S1}\\ I_{S2}\\ I_{S3}\end{bmatrix} \tag{6}$$

with

$$I_{S0} = \frac{1}{\sqrt{3}}\left(I_{S1} + I_{S2} + I_{S3}\right) \equiv 0$$

$$\lambda_{R0} = \frac{1}{\sqrt{3}}\left(\psi_{R1} + \psi_{R2} + \psi_{R3}\right) \equiv 0$$

By defining the complex variables

$$\begin{aligned} \psi_R &\triangleq \psi_{Ra} + j\psi_{Rb} = |\psi_R|\, e^{j\alpha_\psi} \\ I_S &\triangleq I_{Sa} + jI_{Sb} = |I_S|\, e^{j\alpha_I} \end{aligned} \tag{7}$$

the mathematical model (1) can be expressed for purposes of control design as follows

$$\begin{aligned} J\frac{d}{dt}\omega_R &= \frac{N_p M}{L_R} v_{\omega_R} - b\omega_R - \tau_L \\ \frac{1}{2}L_R\frac{d}{dt}|\psi_R|^2 &= -R_R|\psi_R|^2 + R_R M v_{\Psi_R} + \mathscr{D}_{\Psi_R} \end{aligned} \tag{8}$$

with

$$I_S = \frac{\psi_R}{|\psi_R|^2}\left(v_{\Psi_R} + jv_{\omega_R}\right) \tag{9}$$

In (8), possible bounded additional disturbances could be considered like $\mathscr{D}_{\Psi_R}$.

Notice that magnetic fluxes can be estimated on-line as proposed by the authors in previous contributions [16], [34]. In contrast, the robust adaptive neural-network control design objectives introduced in this article are the following:

i. Incorporate suppression capabilities of uncertain oscillatory torque disturbances with multiple frequencies in electric current controller signals. Theoretical mathematical modelling errors and parametric uncertainties are furthermore considered.

ii. Accurate tracking of velocity and flux reference trajectories planned for the operation of the induction motor system under influence of unknown oscillatory torque has to be simultaneously performed.

IV. A NEURAL SLIDING-MODE CONTROL APPROACH

A new induction motor control design strategy based on sliding modes and B-spline artificial neural networks is presented in this section. Auxiliary controllers v_{ω_R} and v_Ψ in (8) and (9) are established.

Consider the sliding surface coordinate functions

$$\begin{aligned} \sigma_{\omega_R} &= e_{\omega_R} + \beta_{\omega_R}\int_{t_0}^{t} e_{\omega_R}(\lambda)\, d\lambda \\ \sigma_{\Psi_R} &= e_{\Psi_R} + \beta_{\Psi_R}\int_{t_0}^{t} e_{\Psi_R}(\lambda)\, d\lambda \end{aligned} \tag{10}$$

where the reference trajectory tracking errors are given by

$$e_{\omega_R} = \omega_R - \omega_R^\star, \quad e_{\Psi_R} = \Psi_R - \Psi_R^\star \tag{11}$$

Here $\omega_R^\star(t)$ stands for some smooth reference profile predefined for the angular speed ω_R. $\Psi_R^\star(t)$ denotes the reference trajectory planned for $\Psi_R = |\psi_R|^2$.

Globally exponentially stable closed-loop reference tracking error dynamics can be thus specified as

$$\begin{aligned} \frac{d}{dt}e_{\omega_R} + \beta_{\omega_R}e_{\omega_R} &= 0 \\ \frac{d}{dt}e_{\Psi_R} + \beta_{\Psi_R}e_{\Psi_R} &= 0 \end{aligned} \tag{12}$$

with design parameters: $\beta_{\omega_R},\ \beta_{\Psi_R} > 0$.

Auxiliary controllers can be then synthesized as

$$\begin{aligned} v_{\omega_R} = \frac{JL_R}{N_p M}\Bigg[&\frac{d}{dt}\omega_R^\star - \beta_{\omega_R}e_{\omega_R} + \frac{b}{J}\omega_R \\ &-k_{\omega_R}\sigma_{\omega_R} - W_{\omega_R}\mathrm{sign}\left(\sigma_{\omega_R}\right)\Bigg] \\ v_{\Psi_R} = \frac{L_R}{2R_R M}\Bigg[&\frac{d}{dt}\Psi_R^\star - \beta_{\Psi_R}e_{\Psi_R} + \frac{2R_R}{L_R}\Psi_R \\ &-k_{\Psi_R}\sigma_{\Psi_R} - W_{\Psi_R}\mathrm{sign}\left(\sigma_{\Psi_R}\right)\Bigg] \end{aligned} \tag{13}$$

with $k_{\omega_R},\ k_{\Psi_R} \geq 0$, and discontinuous control action parameters selected as

$$W_{\omega_R} > \frac{1}{J}|\tau_L|, \quad W_{\Psi_R} > \frac{2}{L_R}\left|\mathscr{D}_{\Psi_R}\right| \tag{14}$$

Uncoupled disturbed discontinuous dynamics of the sliding surface coordinate functions are then governed by

$$\frac{d}{dt}\sigma_{\omega_R} = -k_{\omega_R}\sigma_{\omega_R} - W_{\omega_R}\mathrm{sign}\left(\sigma_{\omega_R}\right) - \frac{1}{J}\tau_L \tag{15}$$

$$\frac{d}{dt}\sigma_{\Psi_R} = -k_{\Psi_R}\sigma_{\Psi_R} - W_{\Psi_R}\mathrm{sign}\left(\sigma_{\Psi_R}\right) + \frac{2}{L_R}\mathscr{D}_{\Psi_R} \tag{16}$$

Consider the Lyapunov functions associated with uncoupled dynamics described by (15) and (16)

$$V_{\sigma_{\omega_R}}\left(\sigma_{\omega_R}\right) = \frac{1}{2}\sigma_{\omega_R}^2, \quad V_{\sigma_{\Psi_R}}\left(\sigma_{\Psi_R}\right) = \frac{1}{2}\sigma_{\Psi_R}^2 \tag{17}$$

where

$$\begin{aligned} \frac{d}{dt}V_{\omega_R}\left(\sigma_{\omega_R}\right) &\leq -k_{\omega_R}\sigma_{\omega_R}^2 - \left(W_{\omega_R} - \frac{1}{J}|\tau_L|\right)\left|\sigma_{\omega_R}\right| \\ &< 0, \quad \text{for } W_{\omega_R} > \frac{1}{J}|\tau_L|,\ \sigma_{\omega_R} \neq 0 \end{aligned} \tag{18}$$

$$\begin{aligned} \frac{d}{dt}V_{\sigma_{\Psi_R}}\left(\sigma_{\Psi_R}\right) &\leq -k_{\Psi_R}\sigma_{\Psi_R}^2 - \left(W_{\Psi_R} - \frac{2}{L_R}\left|D_{\Psi_R}\right|\right)\left|\sigma_{\Psi_R}\right| \\ &< 0, \quad \text{for } W_{\Psi_R} > \frac{2}{L_R}\left|D_{\Psi_R}\right|,\ \sigma_{\Psi_R} \neq 0 \end{aligned} \tag{19}$$

Therefore sliding surfaces $\sigma_{\omega_R} = 0$ and $\sigma_{\Psi_R} = 0$ are reachable in finite time [35]. Tracking of reference trajectories is then performed as follows

$$\lim_{t\to\infty}\omega_R = \omega_R^\star(t), \quad \lim_{t\to\infty}\Psi_R = \Psi_R^\star(t) \tag{20}$$

Furthermore, for operational scenarios in which the system parameters are completely unknown the following auxiliary controllers are proposed:

$$\begin{aligned} v_{\omega_R} &= -\widetilde{k}_{\omega_R}\sigma_{\omega_R} - \widetilde{W}_{\omega_R}\mathrm{sign}\left(\sigma_{\omega_R}\right) \\ v_{\Psi_R} &= -\widetilde{k}_{\Psi_R}\sigma_{\Psi_R} - \widetilde{W}_{\Psi_R}\mathrm{sign}\left(\sigma_{\Psi_R}\right) \end{aligned} \tag{21}$$

with $\widetilde{k}_{\omega_R},\ \widetilde{k}_{\Psi_R} \geq 0$, and

$$\widetilde{W}_{\omega_R} > |\widetilde{\tau}_L|, \quad \widetilde{W}_{\Psi_R} > \left|\widetilde{\mathscr{D}}_{\Psi_R}\right| \tag{22}$$

Unknown disturbances $\widetilde{\tau}_L$ and $\widetilde{\mathscr{D}}_{\Psi_R}$ are given by

$$\widetilde{\tau}_L = \beta_{\omega_R}e_{\omega_R} - \frac{d}{dt}\omega_R^\star - \frac{b}{J}\omega_R - \frac{1}{J}\tau_L$$

$$\widetilde{\mathscr{D}}_{\Psi_R} = \beta_{\Psi_R} e_{\Psi_R} - \frac{d}{dt}\Psi_R^{\star} - \frac{2R_R}{L_R}\Psi_R + \frac{2}{L_R}\mathscr{D}_{\Psi_R} \tag{23}$$

The significatively disturbed, controlled uncoupled discontinuous dynamics of sliding surface coordinate functions are now described by

$$\begin{aligned}\frac{d}{dt}\sigma_{\omega_R} &= -\widetilde{k}_{\omega_R}\sigma_{\omega_R} - \widetilde{W}_{\omega_R}\text{sign}\left(\sigma_{\omega_R}\right) + \widetilde{\tau}_L \\ \frac{d}{dt}\sigma_{\Psi_R} &= -\widetilde{k}_{\Psi_R}\sigma_{\Psi_R} - \widetilde{W}_{\Psi_R}\text{sign}\left(\sigma_{\Psi_R}\right) + \widetilde{\mathscr{D}}_{\Psi_R}\end{aligned} \tag{24}$$

where

$$\begin{aligned}\tilde{\tau}_L &= \beta_{\omega_R} e_{\omega_R} - \frac{d}{dt}\omega_R^{\star} - \frac{b}{J}\omega_R - \frac{1}{J}\tau_L \\ \widetilde{\mathscr{D}}_{\Psi_R} &= \beta_{\Psi_R} e_{\Psi_R} - \frac{d}{dt}\Psi_R^{\star} - \frac{2R_R}{L_R}\Psi_R + \frac{2}{L_R}\mathscr{D}_{\Psi_R}\end{aligned} \tag{25}$$

Similarly, first time derivatives of Lyapunov function candidates (17) along system trajectories (24) are given by

$$\begin{aligned}\frac{d}{dt}V_{\omega_R}\left(\sigma_{\omega_R}\right) &\leq -\widetilde{k}_{\omega_R}\sigma_{\omega_R}^2 - \left(\widetilde{W}_{\omega_R} - |\widetilde{\tau}_L|\right)|\sigma_{\omega_R}| \\ &< 0, \quad \text{for } \widetilde{W}_{\omega_R} > |\widetilde{\tau}_L|\,,\ \sigma_{\omega_R} \neq 0\end{aligned} \tag{26}$$

$$\begin{aligned}\frac{d}{dt}V_{\sigma_{\Psi_R}}\left(\sigma_{\Psi_R}\right) &\leq -\widetilde{k}_{\Psi_R}\sigma_{\Psi_R}^2 - \left(\widetilde{W}_{\Psi_R} - \left|\widetilde{D}_{\Psi_R}\right|\right)|\sigma_{\Psi_R}| \\ &< 0, \quad \text{for } \widetilde{W}_{\Psi_R} > \left|\widetilde{D}_{\Psi_R}\right|\,,\ \sigma_{\Psi_R} \neq 0\end{aligned} \tag{27}$$

Hence sliding surfaces $\sigma_{\omega_R} = 0$ and $\sigma_{\Psi_R} = 0$ are also reachable in finite time by implementing controllers (21). Similarly, tracking of velocity and magnetic flux reference trajectories is then achieved: $\omega_R \to \omega_R^{\star}$, $\Psi_R \to \Psi_R^{\star}$. Moreover, B-spline artificial neural networks are integrated to intelligently improve the stringent robust control performance against uncertain complex dynamic external influences, parametric uncertainty and nonlinear mathematical modelling errors. The control parameters are adjustable online from an artificial intelligence perspective in this fashion. Artificial intelligence indeed offers potential opportunities to develop innovations in adaptive optimal nonlinear control design for considerably uncertain operational scenarios.

In an Artificial Neural Network (ANN), a node - neuron or perceptron - constitutes a fundamental unit that receives input, processes it through a mathematical operation, and produces an output. Nodes are structured into layers within the neural network, typically comprising an input layer, one or more hidden layers, and an output layer.

In this context, B-spline Neural Networks (BsNN's) are intelligent agents that can provide to control systems the capability to adjust their performance when facing significant changes in the plant and the operational environment whilst meeting strict controller specifications, such as the minimization of the system output error and the control input effort. Therefore, in spite of the model uncertainty increases as the system complexity does, and the presence of undesired external disturbing signals during system operation might degrade the system performance, BsNN's efficiently holds a progressive learning by means of their learning rule and the update of their synaptic weights allowing a proper system functioning.

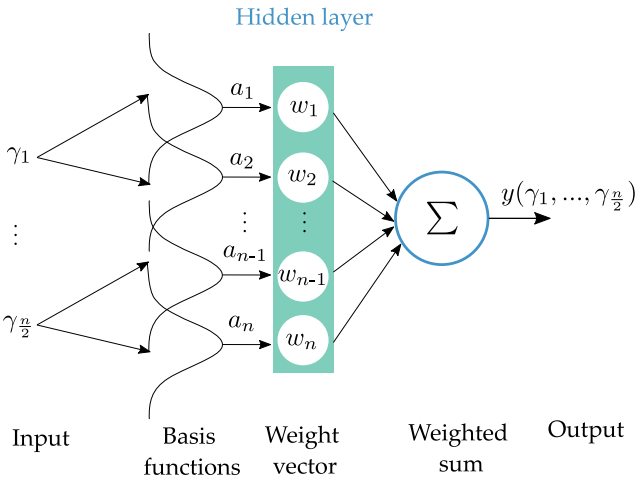

FIGURE 1. Main architecture of a B-spline Neural Network (BsNN).

The presence of unpredictable disturbances may lead to difficulties to perform a satisfactory control of the process or system, then novel designs of complex and more sophisticated controllers is an open research area. In this research, authors propose a novel control approach where a sliding mode-based controller is further enhanced by employing BsNN's for the real-time computation of the control parameters.

In the neuron architecture, the choice of inputs is determined by the close correlation between the output tracking error and the control inputs signals [36]. The neuron output is derived from a weighted linear combination of the transformed inputs. A generalized architecture for a BsNN is depicted in Fig. 1. A couple of basis functions is considered per input signal, $\forall n = 2k : k \in \mathbb{Z}$, where n represents the number of synaptic weights.

In this work, the reference trajectory tracking errors and the sliding surfaces are used as the main inputs signals, and the output is given by

$$y = \mathbf{a}^T\mathbf{w} \tag{28}$$

The weight and basis function outputs (or transformed input) column vectors are given as follows

$$\mathbf{w}^T = [w_1\ w_2 \ldots w_n]\,, \quad \mathbf{a}^T = [a_1\ a_2 \ldots a_n] \tag{29}$$

with

$$\mathbf{w}\,(t) = \mathbf{w}\,(t-1) + \Delta\mathbf{w}\,(t-1) \tag{30}$$

In this study, each control parameter is computed by implementing a BsNN as displayed in Fig. 1. Output tracking errors and sliding surface functions are used as main inputs throughout the simulation experiments. The artificial neuron is continuously trained by using the following instantaneous learning rule:

$$\Delta\mathbf{w}\,(t-1) = \frac{\lambda e\,(t)}{\|\,\mathbf{a}\,(t)\,\|_2^2}\mathbf{a}\,(t) \tag{31}$$

Here $e(t)$ and λ stand for the instantaneous system output tracking error and the learning rate index, respectively. Instantaneous error correction rules allow the update of the weight vector of the network to reduce the error in the output after each training sample is presented to the network. In this sense, adaptation occurs through backward output error propagation [37], [38].

The operation of the BsNN can be furthermore analysed by using a Functional Flow Block Diagram (FFBD) [39]. A scenario in which the output tracking error can be utilized as the correction input signal in the BsNN to compute the control parameters on-line is exemplified in Fig. 2. The measured tracking error is firstly employed as the central input to the neuron and transformed by the B-spline basis functions to get the transformed input vector $\mathbf{a}$ in function block 1.0.

Furthermore, the incorporation of a dead band can enhance the update process and promote the convergence of the learning rule. Specifically, weight factors are either not updated or retained if the error magnitude falls below a specified threshold, as outlined in functions 2.0 and 3.0. Storage of the current weights values is continuously performed for the update stage in the next iteration, as summarized in the function block 4.0. Lastly, the weighted sum is the result of the scalar product of weights and weighted inputs vectors producing the adaptive output. The weights magnitude determines the strength of the connection from each input with the output.

In this research, the on-line computing of the control parameters related to the tracking control for ω_R, based on the tracking error, is carried out by means of the artificial network, adopting the structure presented in Fig. 1. Notwithstanding, in the first case study in the results sections, BsNN's are used effectively for demonstrating the computing of the magnetic flux control design parameters: k_{Ψ_R} and W_{Ψ_R}.

The computational cost of the neuronal outline employed in this research is lower than traditional neural algorithms, such as the multilayer perceptron or radial basis functions. This efficiency stems from the fact that the definition in these networks primarily depends on their base functions, which can be established by understanding the value intervals that may arise in input variables. Furthermore, the continuous and on-line training strategy ensures its constant adaptation to the desired velocity output, mitigating the challenge associated with selecting a training dataset for the neural model, a predicament encountered with the multilayer perceptron during offline training.

The B-spline neural network architecture design consists of the same number of neurons as the computed control design parameters, which varies in each case study. The B-spline basis functions are specified as third-order and constructed over knot vectors. It is important to note that the input is normalized. Additionally, regarding the learning rate, it initially assumes a value within the [0, 2] range for stability purposes [38]. This value undergoes iterative adjustment in small intervals, guided by the measurement of the neural network's dynamic response characteristics. In this research the adopted BsNN structure for case studies are portrayed in Fig. 3.

If λ is close to zero, the learning process becomes sluggish. Conversely, if the value is large, oscillations can arise and grow. In this study, to ensure rapid learning and the convergence of the training rule, a learning rate is set in the range of $(0.001 - 0.5)$ during the simulation experiments, where optimal performance was determined through offline tests. It is proposed that during the update procedure, a dead-band be included to enhance the convergence of the learning rule. The weight factors are not updated if the magnitude of the error is less than 0.1% as

$$\mathbf{w}(t) = \begin{cases} \mathbf{w}(t-1) + \Delta\mathbf{w}(t-1) & \text{if } |e(t)| > 0.001 \\ \mathbf{w}(t-1) & \text{else} \end{cases} \tag{32}$$

The BsNN demonstrates the capability to compute its response in real-time, exploiting a compact structure and a minimal set of fundamental mathematical operations. This characteristic is particularly advantageous for the efficient control in diverse engineering applications. In summary, the design of the B-spline ANN during simulations involves configuring the network architecture and fine-tuning parameters to achieve optimal performance. This iterative process includes determining the number of nodes or neurons, defining the order and number of basis functions, and adjusting connection weights between nodes. Through these simulations, the refinement of these design aspects ensures that the B-spline ANN effectively learns from the gathered data.

The implementation of adaptive control with B-spline neural networks offers a versatile approach that aligns with the demands of complex nonlinear systems. The ability to adapt in real-time, the simply three-layer structure and robustness to uncertainties, positions this methodology as a valuable tool for achieving acceptable control performance in diverse dynamic environments.

Moreover, gradient descent techniques, as the adopted in this work (31), are more suitable for B-spline networks compared to more complex recursive least squares algorithms. These techniques are particularly well-suited for on-line implementations, providing a more efficient and effective alternative in terms of simplicity and performance.

V. CONTROL PERFORMANCE OUTCOMES UNDER CONSIDERABLY DISTURBED OPERATIONAL ENVIRONMENTS

Efficacy of the predefined motion planning tracking control technique based on artificial neural networks and sliding modes for induction or asynchronous motors is furthermore demonstrated in this section through numerical experiments. The Runge-Kutta-Fehlberg method was implemented to solve nonlinear differential equations of the controlled nonlinear dynamics of the electric motor under influence of

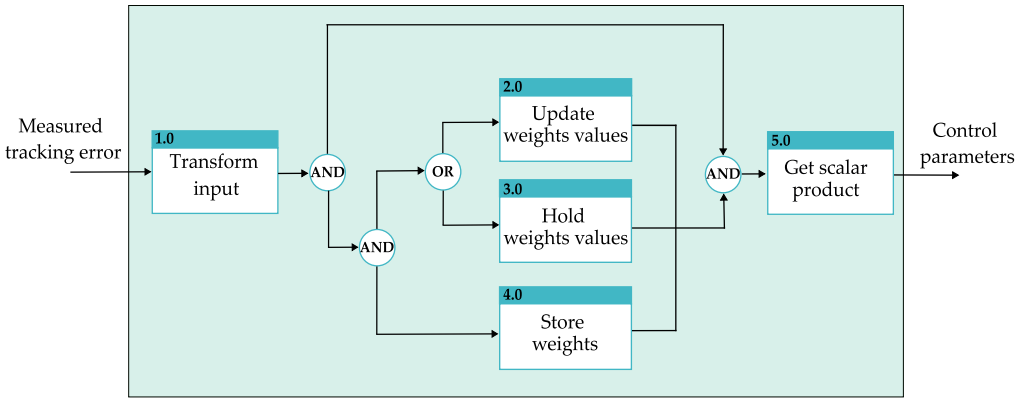

FIGURE 2. Functional flow block diagram of a BsNN.

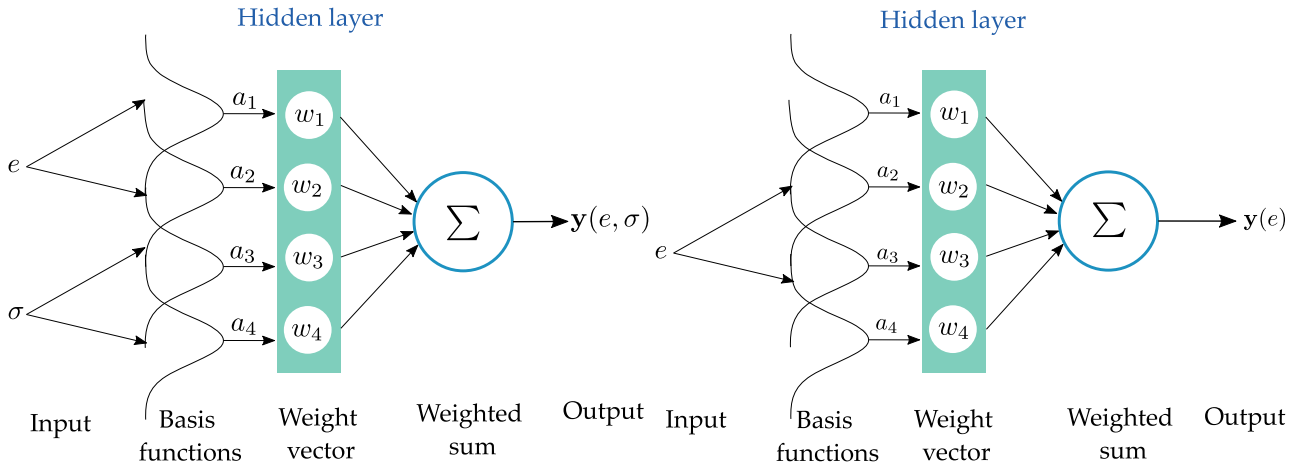

(a) Proposed BsNN structure for case study 1.

(b) Proposed BsNN structure for case studies 2, 3 and 4.

FIGURE 3. Proposed B-spline artificial neural network structures for case studies.

multiple frequency oscillatory torque. A fixed step size of 1 ms was employed in numerical implementations. Values of the parameters of the three-phase asynchronous motor system, with nominal specifications: 500 HP, 2300 V_{RMS} and 60 Hz, are indicated in Table 1 [31].

A general block diagram of the introduced tracking control method is portrayed in Fig. 4. An inner block associated with controllers (13) is displayed in Fig. 4b. In this way, artificial intelligence adaptation capability of the nonlinear induction motor control approach to suppress uncertain multiple-frequency dynamic disturbances using BsNN's and sliding modes is depicted. The control parameters are continually tuned to actively reject possible external uncertain dynamic disturbances. In this section, four case studies are evaluated throughout numeric simulations to highlight the kindness of our outline for facing vibrating load torques and regulating the induction motor towards reference trajectories planned for the angular velocity and magnetic flux. In all the cases, the expressions (36) and (34) are adopted for the smooth transient responses between initial and final operational conditions of

TABLE 1. Electric motor system parameters used in numerical implementations.

Parameter	Value	Unit
X_{ls}	1.206	Ω
X_{lr}	1.206	Ω
X_M	54.02	Ω
R_S	0.262	Ω
R_R	0.187	Ω
J	11.06	kgm^2
b	0.001	Nms

the induction motor system:

$$\Gamma^{\star} = \begin{cases} \Gamma_0 & 0 \le t < T_1 \\ \Gamma_0 + \left(\Gamma_f - \Gamma_0\right) \mathcal{B}_z(t, T_1, T_2) & T_1 \le t \le T_2 \\ \Gamma_f & t > T_2 \end{cases} \tag{33}$$

where Γ_0 and Γ_f stand for the initial and final desired values, respectively. On the other hand, T_1 is the time when the

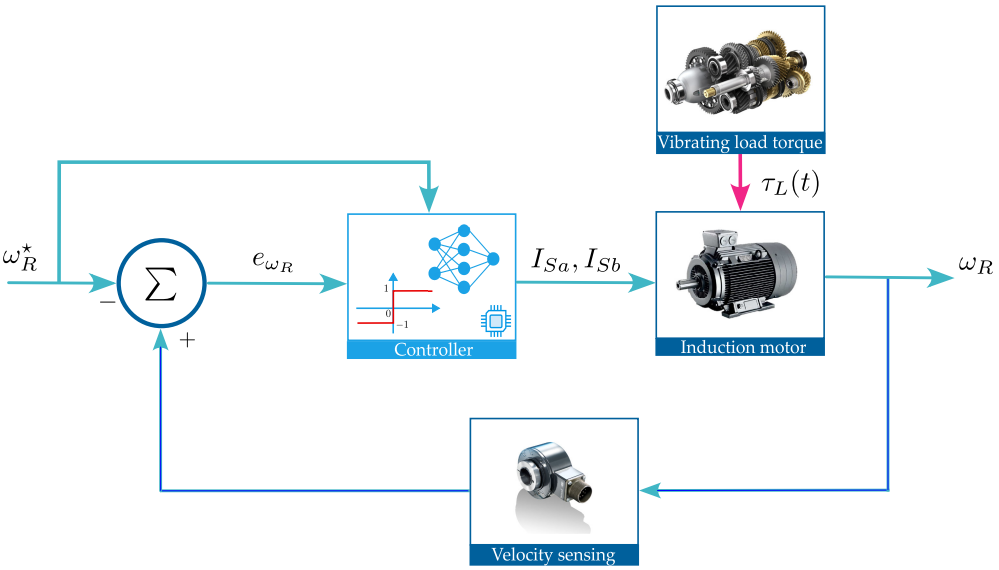

(a) Main components of the induction motor control system under uncertain multiple frequency vibratory torque.

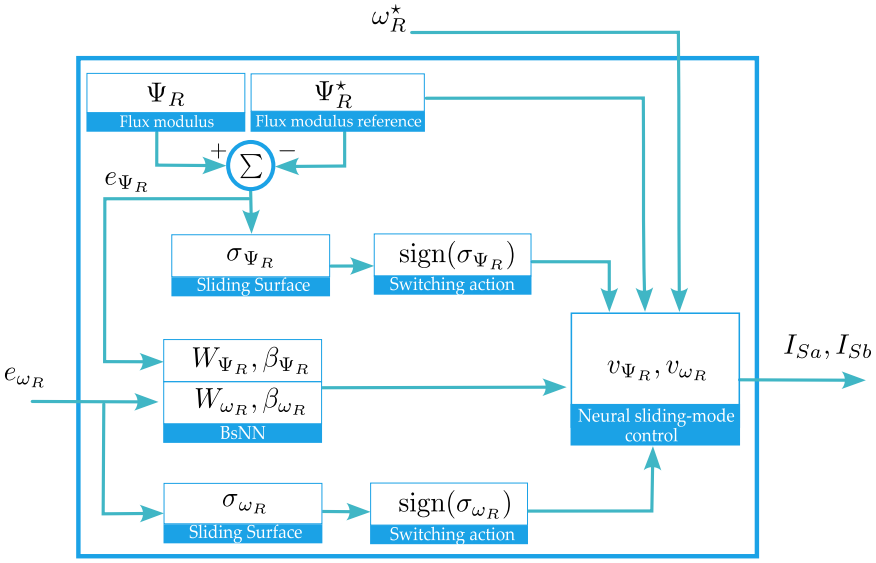

(b) Zooming into the inner controller block to add adaptation capabilities to suppress unknown dynamic disturbances.

FIGURE 4. Overall block diagram of the new proposed adaptive robust control method based on B-spline artificial neural networks and sliding modes.

transition begins and T_2 when finishing. Therefore,

$$\mathcal{B}_z(t, T_1, T_2) = \sum_{k=0}^{n} \mu_k \left(\frac{t - T_1}{T_2 - T_1} \right)^k \tag{34}$$

Here $n = 6$, $\mu_1 = 252$, $\mu_2 = 1050$, $\mu_3 = 1800$, $\mu_4 = 1575$, $\mu_5 = 700$, $\mu_6 = 126$.

A. CASE STUDY 1: UNPERTURBED ANGULAR VELOCITY TRACKING

In this experiment the BsNN structure portrayed in Fig. 3a is adopted in an unperturbed tracking scenario while implementing controllers (13). The control parameters k_i, W_i and β_i, $i = \omega_R, \Psi_R$, are on-line computed by the B-spline neural mechanism where the tracking error e_i and σ_i are used as the inputs. A satisfactory closed-loop tracking of the motor velocity reference trajectory by implementing the neural sliding-mode control approach can be observed in Fig. 5. Moreover, it can be appreciated from Fig. 6 the behaviour of the computed control parameters by using the BsNN which are adjusted according to the tracking error evolution.

In this control method, the initial design considers the current operating conditions of the system, structure, characteristics of the inputs and its response. However, its adaptive nature allows the neural network to learn the

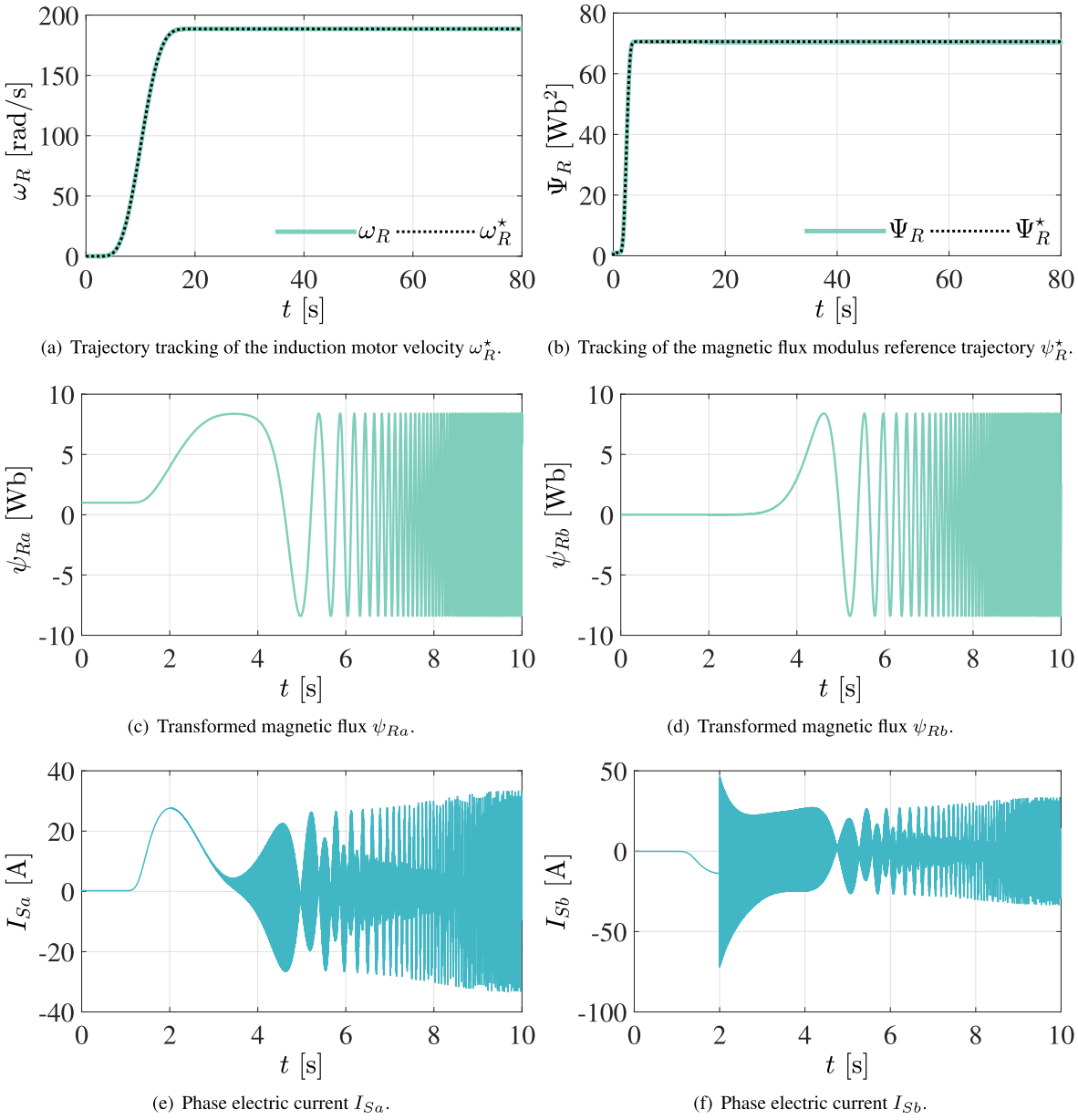

(a) Trajectory tracking of the induction motor velocity $\omega_R^\star$.

(b) Tracking of the magnetic flux modulus reference trajectory $\psi_R^\star$.

(c) Transformed magnetic flux ψ_{Ra}.

(d) Transformed magnetic flux ψ_{Rb}.

(e) Phase electric current I_{Sa}.

(f) Phase electric current I_{Sb}.

FIGURE 5. **Closed-loop induction motor performance for the unperturbed scenario.**

performance of the system and update the control signals as a consequence of the possible modification of the structure, inputs and environment. In this sense, it can be considered that despite the fact that a large number of operating conditions, parametric variations in the system or in its environment were not taken into account in the design of the neural controller, the same learning and updating of the weights will allow consider aspects in future control signals to ensure satisfactory performance in a wide range of actual operating conditions.

The training data includes the transient and steady-state response of the system. One of the advantages of the proposed neural controller is that these data can originate from either an exact or approximate mathematical model or, alternatively, from measured data of the real system (inputs, outputs, control signals, etc.). Besides, in the proposed scheme, four base functions have been employed, two for the error input, and two for the sliding surface.

The knot vectors points of the base functions are proposed as $[-10\ -4\ 2\ 8]$, $[-8\ 4\ 2\ 6]$ for the tracking error, and $[-5\ -3\ -1\ 1]$, $[-2.5\ -0.5\ 1.5\ 3.5]$ for the sliding surface input signal. This definition was developed in the offline training stage by experimentally testing some control parameters values. However, all cases remained within a range of -10 to 10, aiming to ensure that changes in the output of the base functions concerning the input signal were

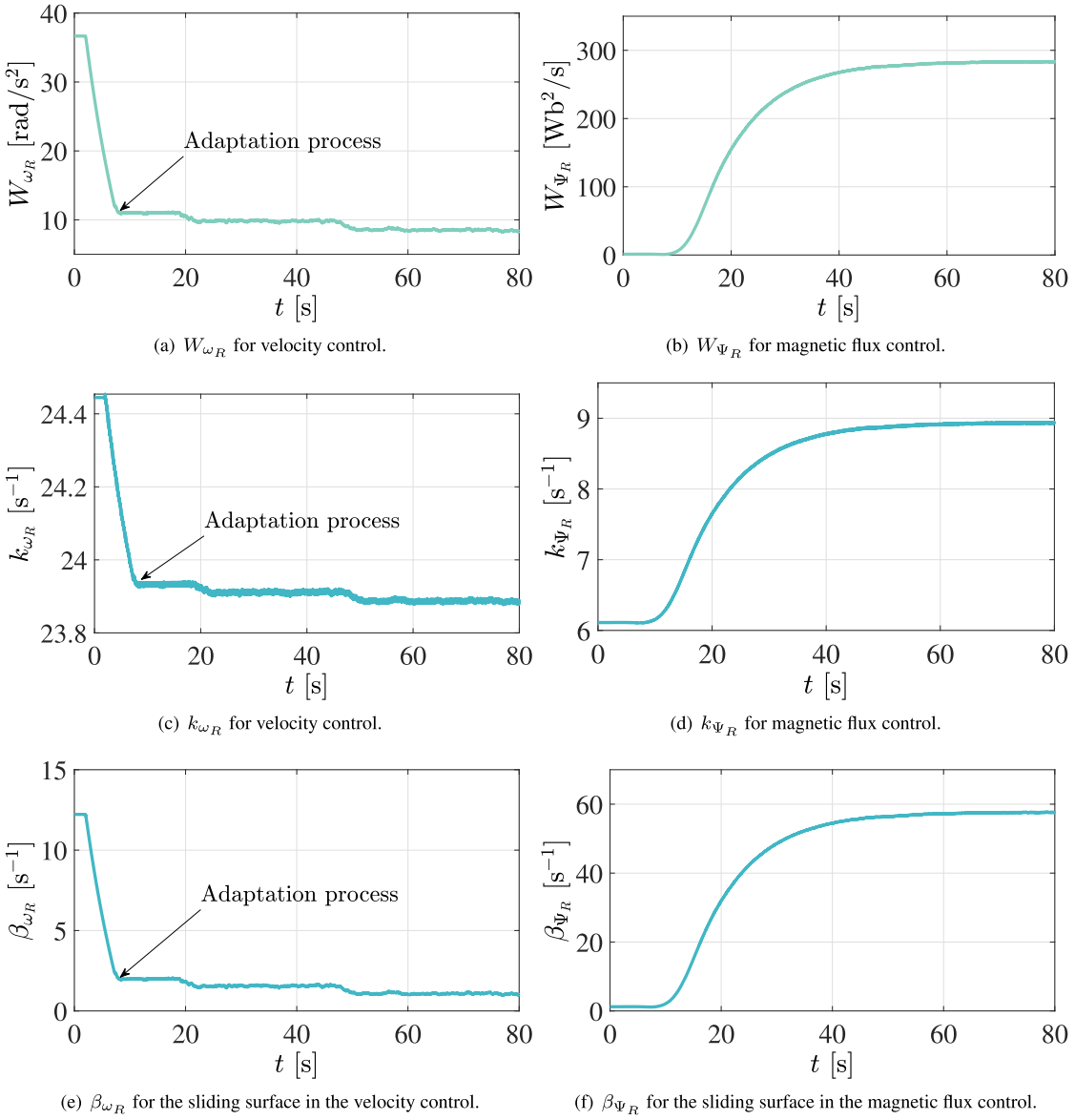

(a) W_{ω_R} for velocity control.

(b) W_{Ψ_R} for magnetic flux control.

(c) k_{ω_R} for velocity control.

(d) k_{Ψ_R} for magnetic flux control.

(e) β_{ω_R} for the sliding surface in the velocity control.

(f) β_{Ψ_R} for the sliding surface in the magnetic flux control.

FIGURE 6. Adaptive control parameters in case study 1 for robust induction motor control.

not too abrupt, and consequently, the output of the neural network.

B. CASE STUDY 2: SINGLE FREQUENCY LOAD TORQUE

For purposes of closed-loop performance assessment, in the second scenario, the velocity trajectory tracking is evaluated when the induction motor is subjected to a vibrating load torque, 20 seconds after the motor started moving, as shown in From Fig. 7, given by the following expression:

$$\tau_L(t) = \mathcal{A}\sin(\Omega_L t + \varphi) \tag{35}$$

where

$$\mathcal{A} = \begin{cases} 0 & 0 \le t \le 20 \\ F\left[1 - e^{-0.5(t-20)}\right] & 20 < t \le 55 \\ F\left[e^{-0.1(t-55)}\right] & t > 55 \end{cases} \tag{36}$$

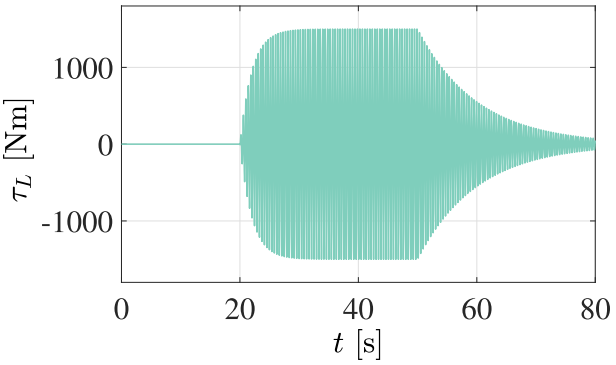

FIGURE 7. Single frequency oscillatory load torque for the second case study.

with $F = 1500$ Nm, $\Omega_L = 15$ rad/s, $\varphi = \frac{\pi}{4}$ rad and t is given in seconds. From Fig. 7 it can be appreciated that

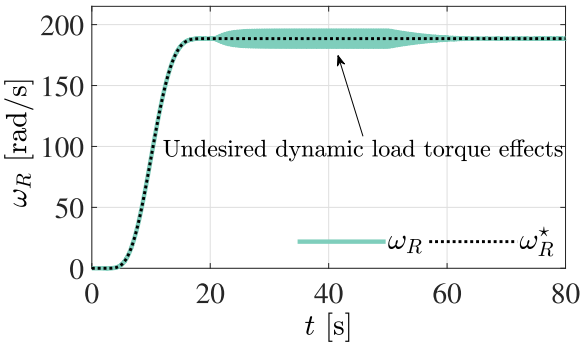

(a) Trajectory tracking of the induction motor velocity using fixed k_{ω_R} and W_{ω_R} control parameters.

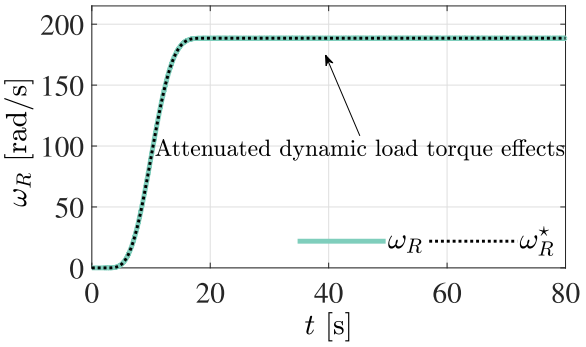

(b) Trajectory tracking of the induction motor velocity using adaptive k_{ω_R} and W_{ω_R} control parameters

FIGURE 8. **Closed-loop induction motor performance in case study 2.**

the undesired vibrating load torque starts to vanishing after 35 seconds from when it was applied.

It is worth to mention that the first controller in (13) is employed in this operation scenario where the BsNN is used for computing the parameters W_{ω_R}, k_{ω_R} and β_{ω_R} as portrayed in Fig. 3b. In this case study arbitrary low gain values are considered for highlighting the effectiveness of the BsNN for adapting different operation scenarios in contrast with the fixed picked values. In this way, it is also corroborated that the off-line training stage of the BsNN's can be efficiently employed for tuning of the fixed control parameters. Learning rate values λ of 0.43, 0.09 and 0.0046, for computing the parameters W_{ω_R}, k_{ω_R} and β_{ω_R}, have been adopted in this scenario.

In Fig. 8 and Fig. 9 it is portrayed a satisfactory system performance by using the proposed control method, where in spite of using relatively low values of the control gains, they are properly on-line adjusted by the neural network. Besides, the effects of the single frequency oscillatory load torque are acceptably attenuated while a proper trajectory tracking of the planed velocity reference is achieved.

To further demonstrate the relevance of including the continuously training capability in the BsNN, it is presented results for the fixed, adaptive, and optimized values of the control parameters for a second comparative analysis in the second case study, where the system is subjected to changes in the velocity reference trajectory, as depicted in Fig. 10. Besides, the time span has been extended to 130 seconds for purposes of illustrating the system's proper operation through the time.

First, consider the scenario when control gains are updated on-line by the BsNN's. Observing from Figs. 11a, 11c and 11e, it is evident that the parameters reach an optimized value after the second change in the velocity reference, transitioning from 188.5 rad/s to 100 rad/s. In this manner, the comparison of system responses is conducted by contrasting the initial, final and adaptive control parameters values computed by the BsNN's.

It is worth noting that although optimized values in the initial scenario may facilitate proper system functioning, such stability is not guaranteed in uncontrolled scenarios where operational conditions involve constant and unpredictable load torques affecting system behaviour, as depicted in the tracking error plots in Fig. 10b, 10d and 10f. Thus, it becomes evident from the figures that real-time updates of the control parameters further enhance the system's capabilities.

The system performance evaluations, in this section and in the case study 4, are conducted using diverse index criteria [40], [41], including the Integral Squared Error (ISE), the Integral Time multiplied Squared Error (ITSE), the Integral Absolute Error (IAE), the Integral Time multiplied Absolute Error (ITAE), and the Root Mean Square Error (RMSE), which is a widely used metric for assessing the accuracy of predictions or control system performance.

The bar graphs shown in Fig. 12 compare the system performance for the second comparative analysis in the second case study. These results provide a comprehensive insight into the controllers' effectiveness, with a particular emphasis on the adaptive controller's superior performance.

From a control theory perspective, the ITAE index is highly sensitive to sustained deviations from the desired output, as it penalizes errors more heavily over time. The adaptive controller demonstrated a substantially lower ITAE value of 430.5, compared to 8883.4 for the fixed controller and 1099.5 for the optimized controller. This indicates that the adaptive controller properly reduce long-term errors, thereby achieving a better reference trajectory tracking.

The ISE index, which emphasizes the magnitude of errors, showed that the adaptive controller achieved an exceptionally low value of 7.4, while the fixed and optimized controllers recorded 923.4 and 18.2, respectively. This suggests that the adaptive controller is highly effective in minimizing the output tracking error, leading to a more precise and efficient system response.

On the IAE index, the adaptive controller again outperformed the others with a value of 6.1, significantly lower than the fixed controller's 196.1 and the optimized controller's 23.0. Since IAE measures the total accumulated error, the adaptive controller's low IAE value indicates superior performance in reducing overall deviation from the reference.

Finally, the ITSE index, which combines the sensitivity to both error magnitude and error duration, highlighted

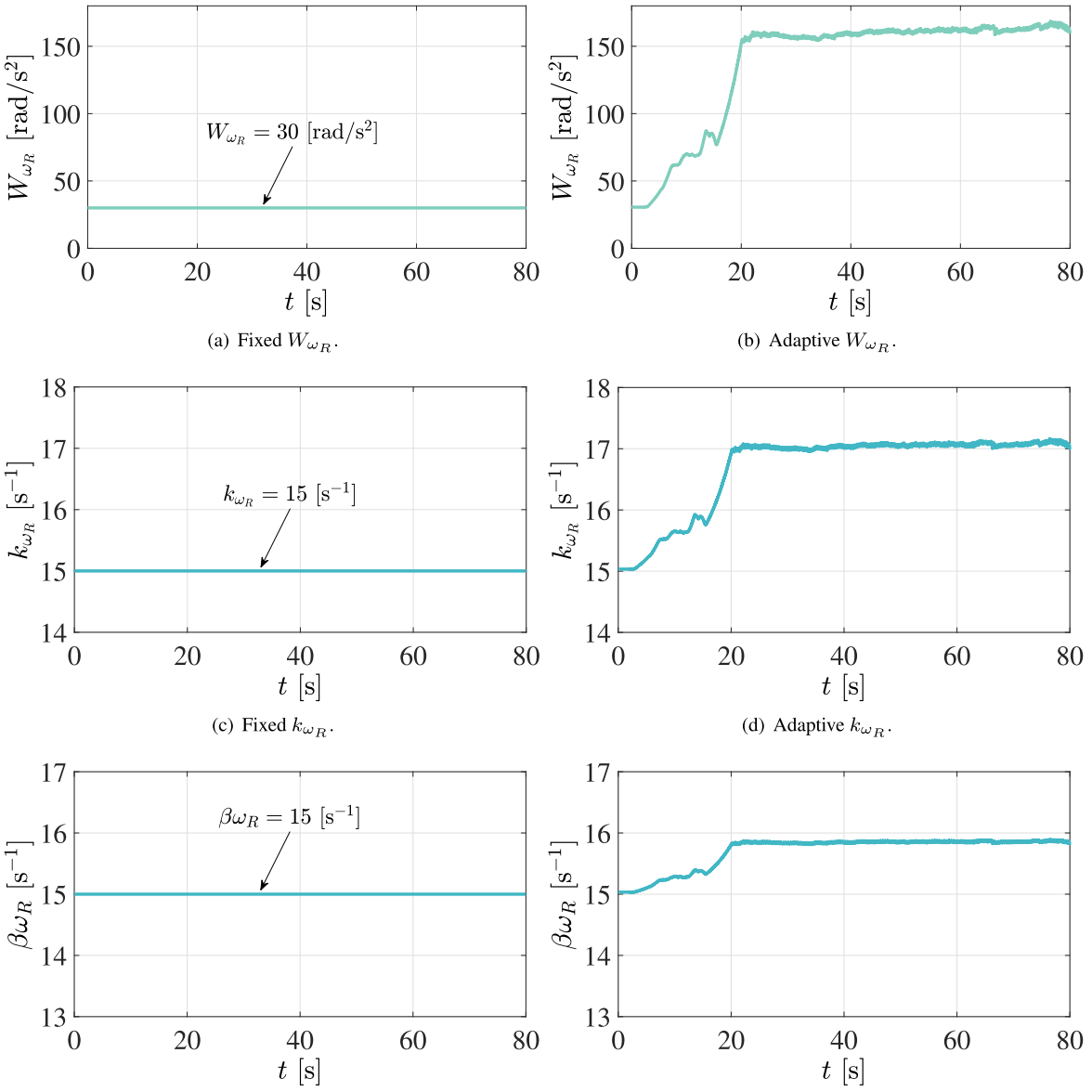

(a) Fixed W_{ω_R}.

(b) Adaptive W_{ω_R}.

(c) Fixed k_{ω_R}.

(d) Adaptive k_{ω_R}.

(e) Fixed β_{ω_R} control parameter used in the sliding surface.

(f) Adaptive β_{ω_R} control parameter used in the sliding surface.

FIGURE 9. Trajectory tracking control parameters in case study 2.

an important improvement with the adaptive controller achieving a value of 131.5, compared to 13973.3 for the fixed controller and 548.4 for the optimized controller. The adaptive controller's low value emphasize its ability to effectively manage both transient and steady-state performance, minimizing both the amplitude and duration of tracking errors.

The presented results consistently emphasize the adaptive controller's capability in minimizing the tracking error and improving the overall operation of the induction motor system. It exhibits exceptional ability to dynamically adjust to changing conditions and disturbances, thereby achieving remarkable efficiency in the control system.

C. CASE STUDY 3: MULTIPLE FREQUENCY LOAD TORQUE

The accuracy and responsiveness of induction motor control are advanced by integrating B-spline neural networks into sliding mode robust controllers. The adaptability of B-spline neural networks is leveraged to enhance the controller's ability to adapt promptly and effectively to fluctuations, disturbances, and varying conditions during motor operation. This integration leads to controllers that understand motor behaviour nuances and respond swiftly to dynamic changes, even in the absence of a precise system dynamical model.

The overall performance of induction motor control systems is significantly enhanced by this collective improvement, making it valuable for practical applications in control

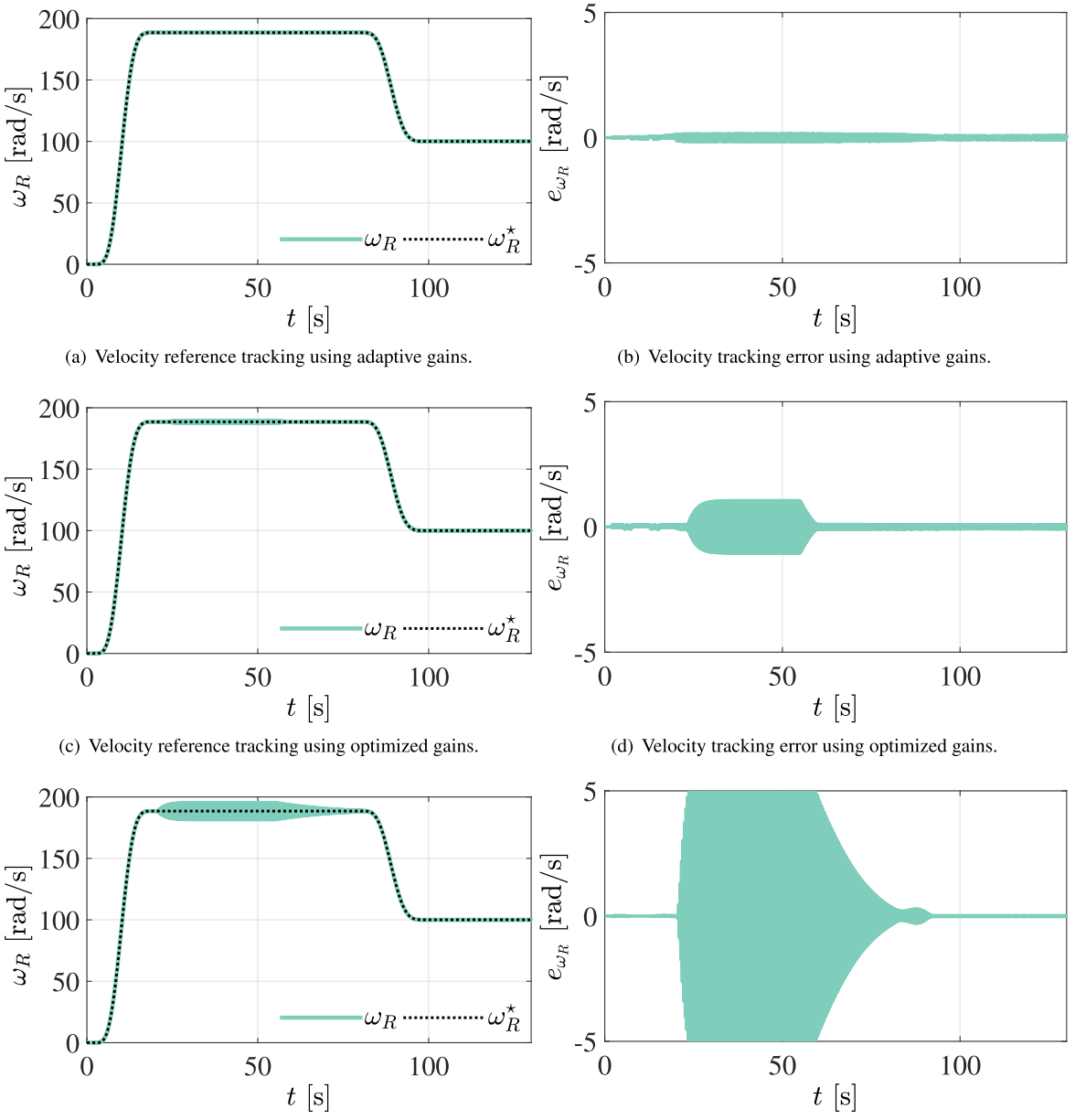

(a) Velocity reference tracking using adaptive gains.

(b) Velocity tracking error using adaptive gains.

(c) Velocity reference tracking using optimized gains.

(d) Velocity tracking error using optimized gains.

(e) Velocity reference tracking using fixed gains.

(f) Velocity tracking error using fixed gains.

FIGURE 10. Velocity reference tracking for the second comparative analysis in case study 2.

engineering. For this case study, it is intentionally exposed to the controlled system to a critical scenario where it is assumed that information from system parameters is not available, thus the selection of control parameters in expression (21) are computed on-line by the BsNN. Thus, arbitrary fixed and initial adaptive control parameter values ($\widetilde{k}_{\omega_R} = 180$ s^{-1} and $\widetilde{W}_{\omega_R} = 550$ rad/s^2) have been selected to highlight how the adaptive approach can be used for the off-line tuning of control parameters as well.

Additionally, a multiple frequency load vibrating torque is intentionally injected after 20 seconds the simulation starts, and stopped at a time $t = 40$ s, as portrayed in Fig. 13, and is given by

$$\tau_L(t) = \sum_{i=1}^{4} \overline{T}_i \tag{37}$$

with

$$\overline{T}_i(t) = \tau_i \sin(\Omega_i t + \varphi_i) + \overline{\tau}_i \sin\left[\left(\Omega_i + \overline{\Omega}_i\right)\frac{t}{2}\right] \sin\left[\left(\Omega_i - \overline{\Omega}_i\right)\frac{t}{2}\right] \tag{38}$$

where the oscillatory load torque parameters are summarized in Table 2.

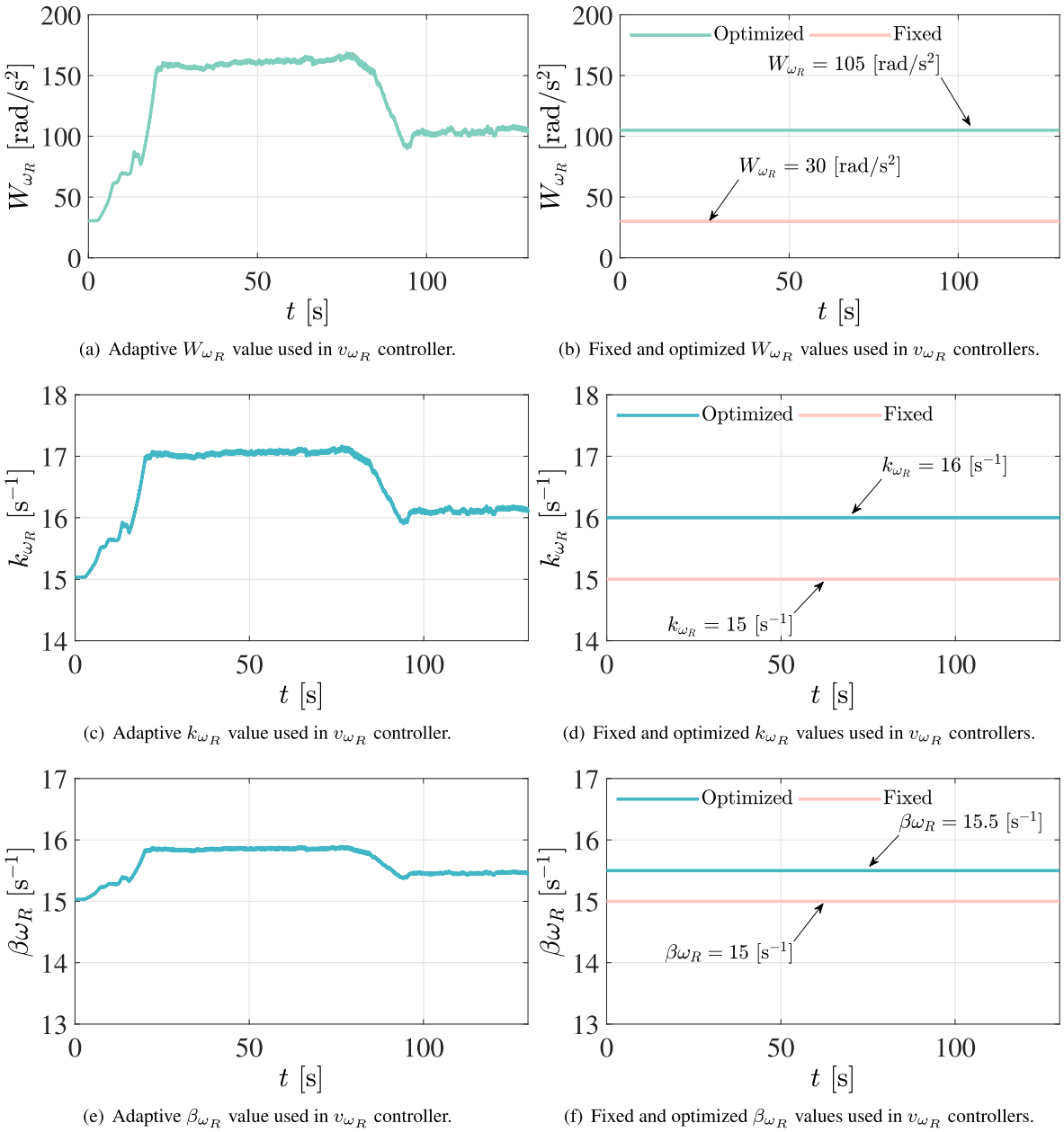

(a) Adaptive W_{ω_R} value used in v_{ω_R} controller.

(b) Fixed and optimized W_{ω_R} values used in v_{ω_R} controllers.

(c) Adaptive k_{ω_R} value used in v_{ω_R} controller.

(d) Fixed and optimized k_{ω_R} values used in v_{ω_R} controllers.

(e) Adaptive β_{ω_R} value used in v_{ω_R} controller.

(f) Fixed and optimized β_{ω_R} values used in v_{ω_R} controllers.

FIGURE 11. Parameter control set for the second comparative analysis in case study 2.

TABLE 2. Parameters of the multiple-frequency oscillatory load torque in the third case study.

Amplitudes Nm	Frequencies rad/s	Phase Angles rad
$\tau_1 = 1500$	$\Omega_1 = 30$	$\varphi_1 = \pi/4$
$\tau_2 = 300$	$\Omega_2 = 28$	$\varphi_1 = \pi/3$
$\tau_3 = 400$	$\Omega_3 = 32$	$\varphi_2 = 2\pi/3$
$\tau_4 = 500$	$\Omega_4 = 34$	$\varphi_3 = 3\pi/4$
$\overline{\tau}_1 = 1500$	$\overline{\Omega}_1 = 30.5$	–
$\overline{\tau}_2 = 400$	$\overline{\Omega}_2 = 27.5$	–
$\overline{\tau}_3 = 300$	$\overline{\Omega}_3 = 32.5$	–
$\overline{\tau}_4 = 200$	$\overline{\Omega}_4 = 33.5$	–

From the yielded results in Fig. 14, it is evident the improved performance of the controlled system by using the proposed robust tracking control scheme in spite of the presence of significant multiple-frequency vibrating load torques. The suitably integration of the Bézier polynomials as reference velocity profiles allows a properly operation from the start to the stop of the electric system motor in different operation scenarios. It is also corroborated a satisfactory performance of the system while acceptable levels of vibration attenuation are achieved as demonstrated previously analytically.

Additionally, low dependence of the system physical parameters information is attained by including the BsNN's in the sliding modes based-control scheme. Finally, it is important to note that the proposed approach can be further

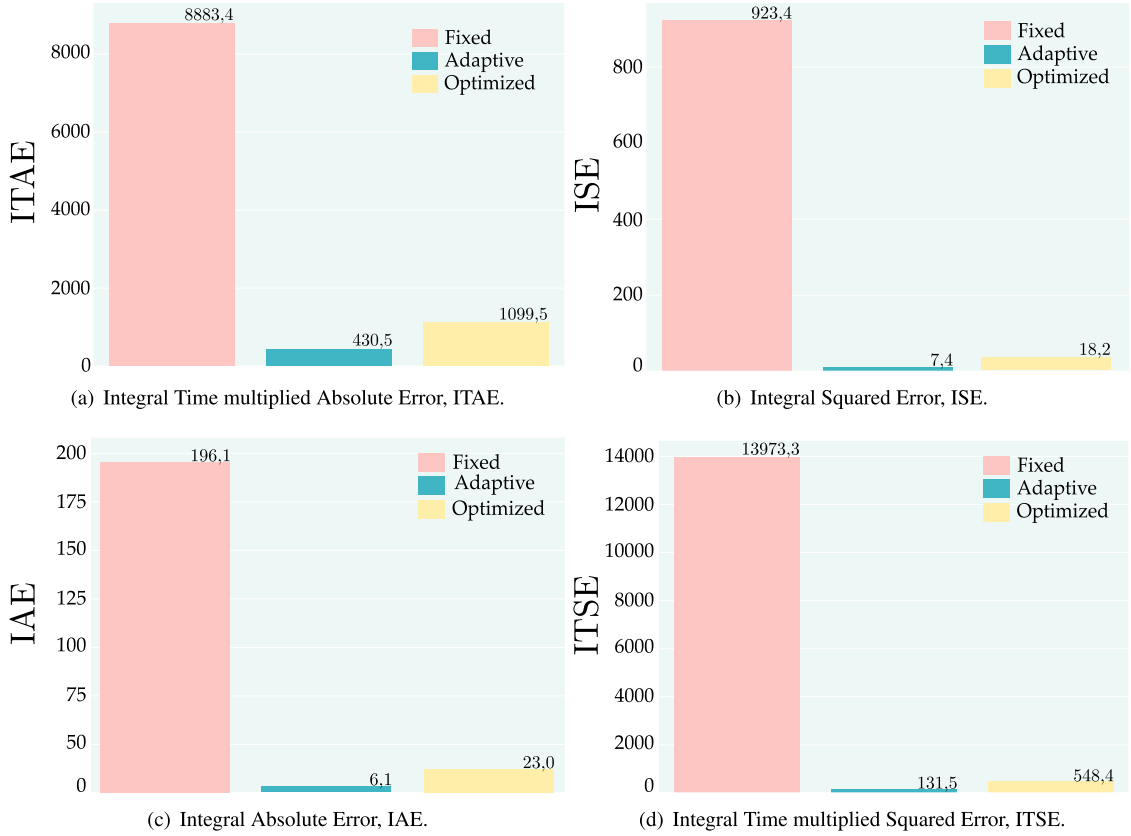

(a) Integral Time multiplied Absolute Error, ITAE.
(b) Integral Squared Error, ISE.
(c) Integral Absolute Error, IAE.
(d) Integral Time multiplied Squared Error, ITSE.

FIGURE 12. System performance evaluation for the second comparative analysis in the second case study.

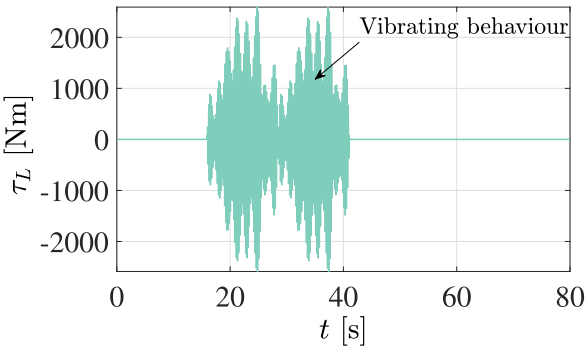

FIGURE 13. Multiple frequency oscillatory load torque for the third operational scenario.

extended to another electric motor architectures where minimal adjustments are required.

Notice from Fig. 15 and Fig. 16 the adaptive capabilities of the control scheme allows to update the control parameters based on information of the tracking error without previous information of the system parameters. It is evident the magnitude of the parameters is greater than the values used when implementing the controller in (13), since the control input address the lack of system information. It is important to highlight that the proposed control approach can handle satisfactory the system uncertainties, unmodeled dynamics and disturbance load torques in an efficient way, as corroborated in the multiple operational simulation scenarios.

Lastly, notice that by implementing the proposed controller it is achieved an acceptable closed-loop performance of the induction motor system which is further improved by the adaptive computation of the control parameters with the BsNN, as demonstrated trough the diverse simulation operational scenarios. Moreover, since induction motors are frequently subjected during its operation to undesired vibrating load torques, it is meaningful to have a control scheme with low dependence on the system model as well as external disturbance information, as required in demanding applications such industrial drives and electric vehicles. Therefore, it is evident that the integration of intelligent agents as individual and multilayer artificial neurons networks in control systems design benefits the optimization and improvement of the closed-loop performance while strict operational requirements are meet.

The performance of BsNN's in control systems is influenced by several sensitive parameters. The number and placement of control points, the degree of B-spline basis functions, and the network architecture impact the system adaptability. Choosing an appropriate learning rate and

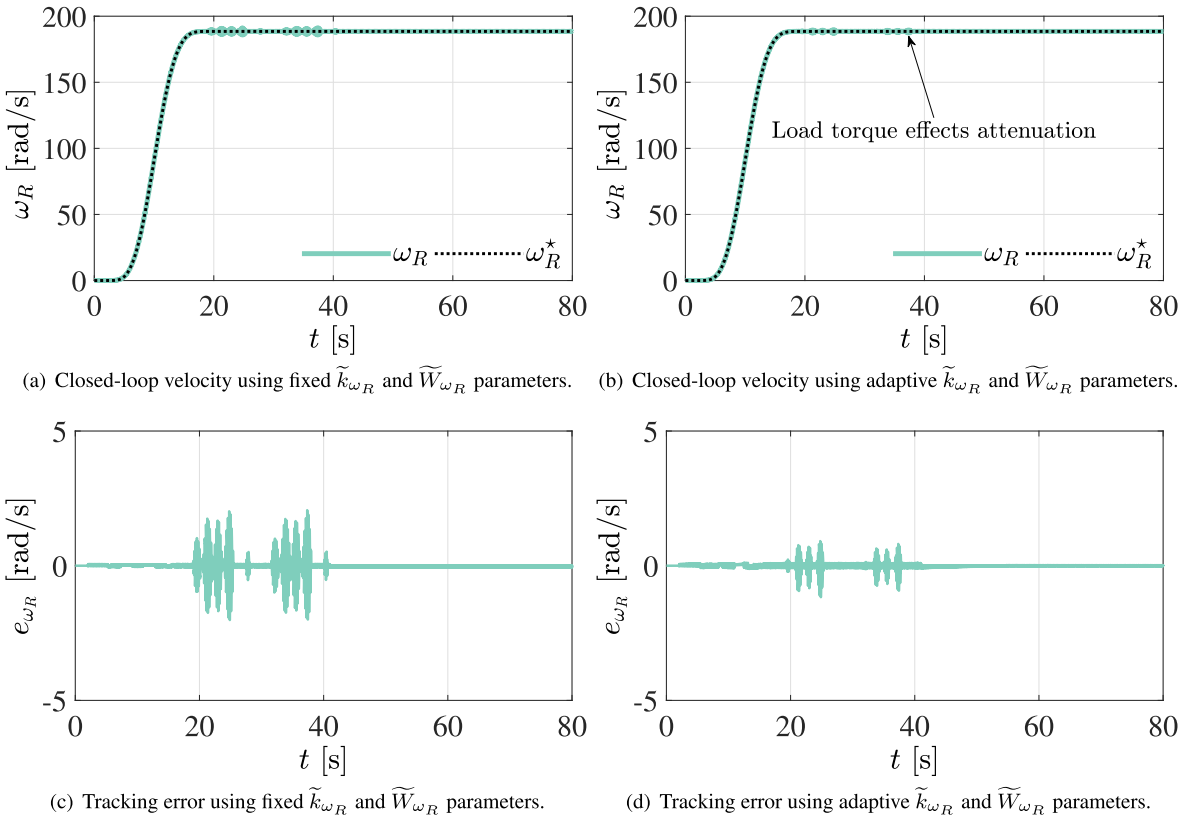

(a) Closed-loop velocity using fixed $\widetilde{k}_{\omega_R}$ and $\widetilde{W}_{\omega_R}$ parameters.

(b) Closed-loop velocity using adaptive $\widetilde{k}_{\omega_R}$ and $\widetilde{W}_{\omega_R}$ parameters.

(c) Tracking error using fixed $\widetilde{k}_{\omega_R}$ and $\widetilde{W}_{\omega_R}$ parameters.

(d) Tracking error using adaptive $\widetilde{k}_{\omega_R}$ and $\widetilde{W}_{\omega_R}$ parameters.

FIGURE 14. Closed-loop induction motor performance for the third scenario.

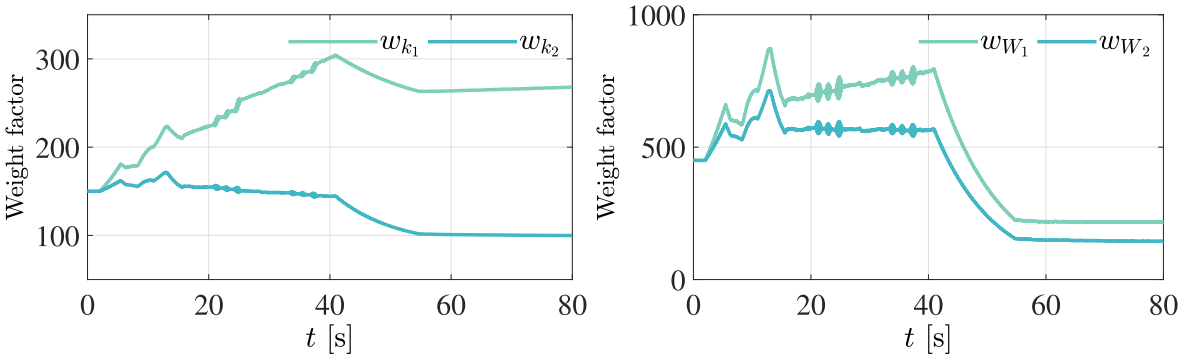

(a) Weight convergence for $\widetilde{k}_{\omega_R}$.

(b) Weight convergence for $\widetilde{W}_{\omega_R}$.

FIGURE 15. Update time-line of the weights for computation of the velocity control parameters by using expression (30) in the third case study.

weight initialization is crucial for preventing overfitting. Balancing these parameters is crucial to avoid slow convergence, ensuring that the BsNN effectively respond to change in the system performance.

D. CASE STUDY 4: EVALUATION ON ADAPTIVE ROBUST B-SPLINE AND NONLINEAR PASSIVITY-BASED CONTROLLERS

The application of the passivity theory in designing controllers for induction motors has demonstrated its effectiveness, as noted in previous research [42]. In this section, it is introduced an additional case study to assess the performance of the proposed approach using the criteria introduced in the second case study. This case study serves as a comparative analysis, highlighting the effectiveness of our approach in contrast to other efficient nonlinear control design methodologies previously proposed in the literature. Here, a time-step simulation of 0.25 ms is adopted for both scenarios as proposed in [16].

The chart depicted in Fig. 17a illustrates the criteria evaluation for the unperturbed scenario. Notice from this figure that each axis indicates the system tracking performance,

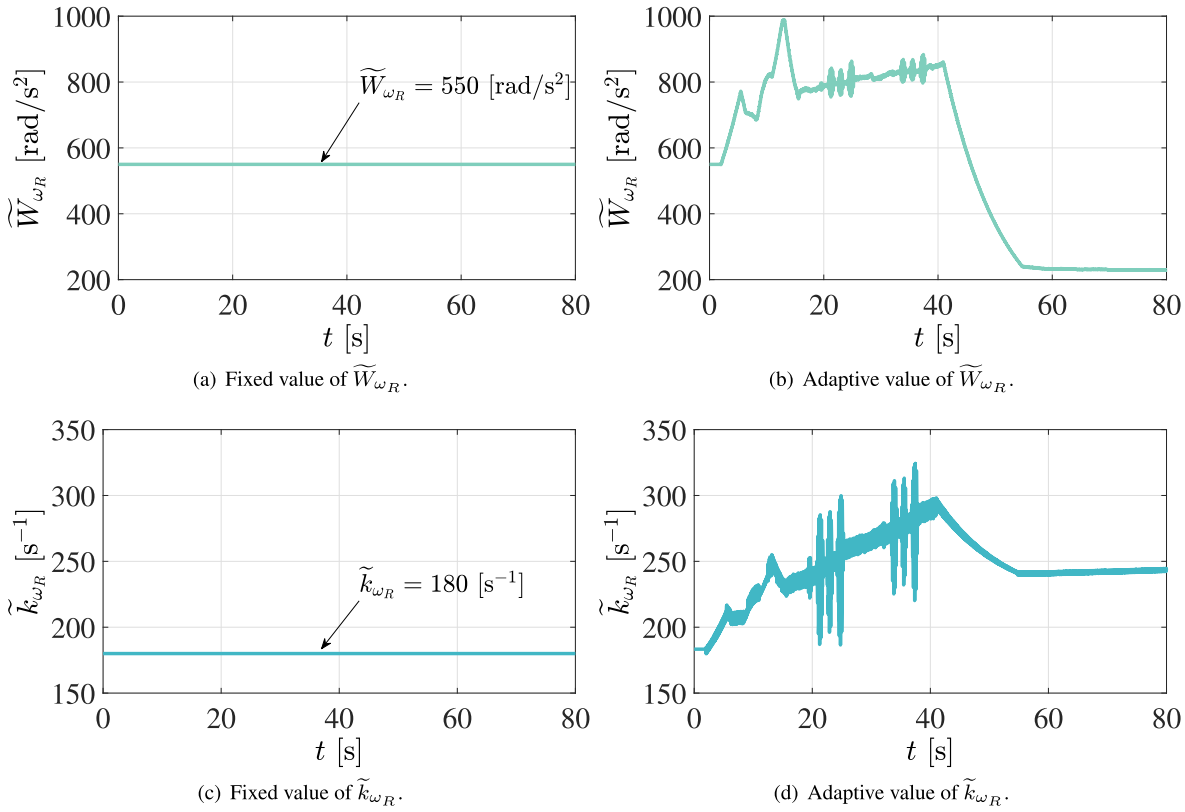

(a) Fixed value of $\widetilde{W}_{\omega_R}$. (b) Adaptive value of $\widetilde{W}_{\omega_R}$.

(c) Fixed value of $\widetilde{k}_{\omega_R}$. (d) Adaptive value of $\widetilde{k}_{\omega_R}$.

FIGURE 16. **Velocity control parameters for the third case study.**

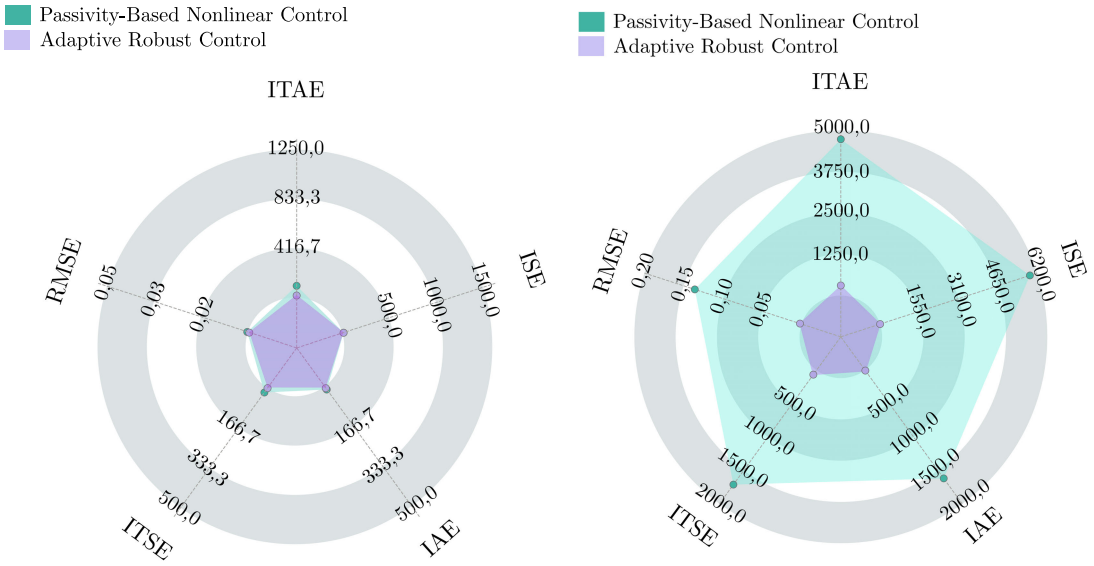

(a) Unperturbed closed-loop system responses. (b) Perturbed closed-loop system responses.

FIGURE 17. **Comparative analysis of the system responses using performance index criteria for the fourth case study.**

demonstrating acceptable system performance using both approaches. On the other hand, Fig. 17b presents the data obtained for criteria evaluation under the influence of a vibrating load torque, highlighting the system's performance. Here, one can appreciate the capability of the proposed approach to effectively drive the system.

Based on the data presented in the radar charts depicted in Fig.17, it is evident that, despite adjustments in the simulation

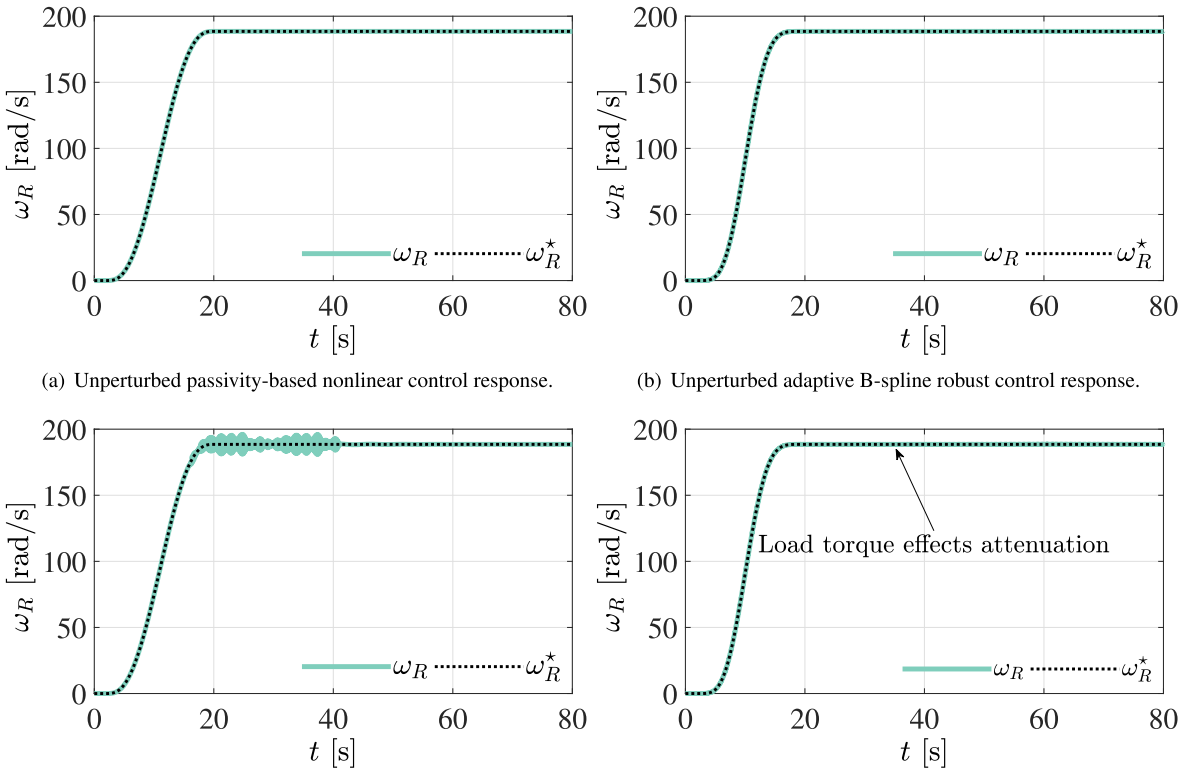

(a) Unperturbed passivity-based nonlinear control response.

(b) Unperturbed adaptive B-spline robust control response.

(c) Perturbed passivity-based nonlinear control response.

(d) Perturbed adaptive B-spline robust control response.

FIGURE 18. Comparative analysis of the velocity motor control in the last case study.

step time, the proposed robust induction motor controller is functioning properly. Furthermore, proficient performance in terms of output tracking velocity error is achieved when implementing the proposed approach, even when the system is subjected to a completely unknown and undesired vibrating load torque, as illustrated in Figure 18.

Observe that by implementing the passivity-based nonlinear controller, it is achieved an acceptable performance. Nevertheless, by using the proposed adaptive robust B-spline controller the system exhibits a superior performance. While the passivity theory offers notable advantages in designing induction motor controllers, it is important to acknowledge that a significant challenge lies in its inherent difficulty in compensating for disturbances. The rigid adherence to the principles of passivity can sometimes limit the controller's ability to effectively mitigate external disturbances, posing a potential limitation in dynamic environments. Addressing this challenge requires careful consideration and additional strategies to enhance the system's resilience to disturbances.

While the integration of B-spline neural networks presents promising advancements in control design, it is essential to acknowledge potential challenges in their implementation. One notable issue lies in the selection of appropriate control parameters. B-spline neural networks demand careful tuning to strike a balance between model complexity and computational efficiency, posing a challenge in achieving an optimal trade-off.

Additionally, an improperly selection of the learning rate value may lead to increased computational costs, making real-time applications challenging. Moreover, ensuring robustness in the face of uncertainties and variations in dynamic systems introduces complexities, as the adaptability of B-spline networks must be carefully managed to avoid overfitting or underfitting issues. Addressing these challenges is crucial for harnessing the full potential of B-spline neural networks in control designs.

These techniques are particularly well-suited for on-line implementations, providing a more efficient and effective alternative in terms of simplicity and performance. For the implementation of adaptive control using B-spline neural networks in a microcontroller, DSPs can be a suitable selection, but careful consideration should be made.

The choice hinges on factors such as the computational prowess to handle the real-time demands of the adaptive control algorithm, the availability of ample memory for storing neural network parameters, and robust peripheral support for seamless interfacing with sensors and communication modules. Equally critical is assessing the development environment, ensuring that the tools provided facilitate efficient programming and debugging.

VI. CONCLUSION

In this article, a new neural adaptive robust nonlinear control design strategy for performing efficient tracking tasks of

predefined motion profiles on uncertain induction motor systems under a wide spectrum of completely unknown, external and internal dynamic disturbances or uncertainties has been proposed. B-spline artificial neural networks, smooth motion reference trajectory tracking and sliding mode theory were utilized to construct the new introduced induction motor control design method. The efficient tracking of smooth operating reference trajectories planned for both the angular velocity and the rotor magnetic flux on the induction motor in substantially disturbed operational environments was demonstrated. Capability of robustness with regard to parametric uncertainty, theoretical dynamic modelling errors and multi-frequency external oscillatory torque perturbations was incorporated in electric current control signals. In contrast to other existing conventional techniques, real-time estimation strategies of system parameters and dynamic disturbances is unnecessary. Analytical and numerical evidence has proved the efficacy of the adaptive trajectory tracking control strategy. A satisfactory control performance without utilizing information of system parameters was corroborated as well. Furthermore, a comparative analysis is carried out using performance criteria for both unperturbed and perturbed scenarios, contrasting with a nonlinear passivity-based controller suggested in the literature. The results demonstrate superior performance with the proposed adaptive robust approach. It can hence be concluded that the introduced adaptive sliding mode neural network nonlinear control strategy represents a very good solution alternative to the problem of external multi-frequency oscillatory perturbation suppression for this controlled nonlinear energy conversion dynamic system, while a tracking of specified motion planning is efficiently fulfilled. It has been confirmed how neural networks and sliding modes theories can be capitalized to enhance the existing body of knowledge about robust tracking control design methodologies of uncertain modern complex engineering systems driven by electric motors. In future research endeavours, it is planned to explore other variants of sliding modes and leverage various artificial intelligence techniques to derive novel solutions for efficient trajectory tracking control problems. This exploration will extend to various types of electric machines and encompass a wide class of multivariable uncertain complex energy conversion nonlinear dynamic systems, where internal and external uncertainties play a crucial role. Additionally, real-time experimental implementation of the introduced approach will be addressed, extending its application to various electric motor configurations.

APPENDIX A
LIST OF ACRONYMS AND SYMBOLS

Acronym	Description
DSP	Digital Signal Processor.
ANN	Artificial Neural Network.
BsNN	B-spline Neural Network.
FFBD	Functional Flow Block Diagram.
ISE	Integral Squared Error.
ITSE	Integral Time multiplied Squared Error.
ITAE	Integral Time multiplied Absolute Error.
IAE	Integral Absolute Error.
RMSE	Root Mean Square Error.

Symbol	Description
ψ_{Ra}, ψ_{Rb}	Transformed magnetic fluxes in rotor.
I_{Sa}, I_{Sb}	Phase electric currents.
N_p	Number of rotor pole pairs.
R_R, R_S	Rotor and stator winding resistances.
L_R, L_S	Rotor and stator inductances.
M	Mutual inductance.
J	Rotor moment of inertia.
τ_L	Mechanical load torque.
ω_R	Rotor angular velocity.
τ_e	Control torque.
$\mathscr{D}_{\Psi_R}$	Bounded disturbances.
$\nu_{\omega_R}, \nu_{\Psi}$	Auxiliary controllers.
$\sigma_{\Psi_R}, \sigma_{\omega_R}$	Sliding surface functions.
e_{ω_R}, e_{Ψ_R}	Trajectory tracking errors.
$\omega_R^\star$	Reference angular rotor speed.
Ψ_R	Magnetic flux modulus.
$\Psi_R^\star$	Reference magnetic flux modulus.
k_{ω_R}, k_{Ψ_R}	Control gain parameters.
$\beta_{\omega_R}, \beta_{\Psi_R}$	Control design parameters.
W_{ω_R}, W_{Ψ_R}	Discontinuous control action parameters.
$\mathcal{B}_z$	Bézier polynomial.
λ	Learning rate index.
$\mathbf{w}$	Weights vector.
$\mathbf{a}$	Basis function outputs vector.
$\mathcal{A}$	Vibrating load torque amplitude.
Ω_L	Vibrating load torque frequency.
φ	Vibrating load torque phase.

ACKNOWLEDGMENT

The authors would like to thank Consejo Nacional de Humanidades, Ciencias y Tecnologías (CONAHCYT) for support provided to developing this work.

REFERENCES

[1] S. Haykin, *Neural Networks and Learning Machines*, 3rd ed. New York, NY, USA: Prentice-Hall, 2009.

[2] S. J. Russell, *Artificial Intelligence: A Modern Approach*. London, U.K.: Pearson, 2010.

[3] A. Saranya and R. Subhashini, "A systematic review of explainable artificial intelligence models and applications: Recent developments and future trends," *Decis. Anal. J.*, vol. 7, Jun. 2023, Art. no. 100230.

[4] I. Kutyauripo, M. Rushambwa, and L. Chiwazi, "Artificial intelligence applications in the agrifood sectors," *J. Agricult. Food Res.*, vol. 11, Mar. 2023, Art. no. 100502.

[5] P. Ong, Y. K. Tan, K. H. Lai, and C. K. Sia, "A deep convolutional neural network for vibration-based health-monitoring of rotating machinery," *Decis. Anal. J.*, vol. 7, Jun. 2023, Art. no. 100219.

[6] D. Ushakov, E. Dudukalov, L. Shmatko, and K. Shatila, "Artificial intelligence as a factor of public transportations system development," *Transp. Res. Proc.*, vol. 63, pp. 2401–2408, Jan. 2022.

[7] J. Wu, X. Wang, Y. Dang, and Z. Lv, "Digital twins and artificial intelligence in transportation infrastructure: Classification, application, and future research directions," *Comput. Electr. Eng.*, vol. 101, Jul. 2022, Art. no. 107983.

[8] F. Un-Noor, S. Padmanaban, L. Mihet-Popa, M. Mollah, and E. Hossain, "A comprehensive study of key electric vehicle (EV) components, technologies, challenges, impacts, and future direction of development," *Energies*, vol. 10, no. 8, p. 1217, Aug. 2017.

[9] D.-D. Tran, M. Vafaeipour, M. El Baghdadi, R. Barrero, J. Van Mierlo, and O. Hegazy, "Thorough state-of-the-art analysis of electric and hybrid vehicle powertrains: Topologies and integrated energy management strategies," *Renew. Sustain. Energy Rev.*, vol. 119, Mar. 2020, Art. no. 109596.

[10] W. N. Caballero, D. R. Insua, and D. Banks, "Decision support issues in automated driving systems," *Int. Trans. Oper. Res.*, vol. 30, no. 3, pp. 1216–1244, May 2023.

[11] G. Bhatti, H. Mohan, and R. R. Singh, "Towards the future of smart electric vehicles: Digital twin technology," *Renew. Sustain. Energy Rev.*, vol. 141, May 2021, Art. no. 110801.

[12] D. Gunning and D. Aha, "DARPA's explainable artificial intelligence (XAI) program," *AI Mag.*, vol. 40, no. 2, pp. 44–58, Jun. 2019.

[13] Y. Xing and C. Lv, "Dynamic state estimation for the advanced brake system of electric vehicles by using deep recurrent neural networks," *IEEE Trans. Ind. Electron.*, vol. 67, no. 11, pp. 9536–9547, Nov. 2020.

[14] F. Pretagostini, L. Ferranti, G. Berardo, V. Ivanov, and B. Shyrokau, "Survey on wheel slip control design strategies, evaluation and application to antilock braking systems," *IEEE Access*, vol. 8, pp. 10951–10970, 2020.

[15] P. Mallozzi, P. Pelliccione, A. Knauss, C. Berger, and N. Mohammadiha, "Autonomous vehicles: State of the art, future trends, and challenges," in *Automotive Systems and Software Engineering: State of the Art and Future Trends*. Springer, 2019, pp. 347–367.

[16] F. Beltran-Carbajal, "A harmonic vibration suppression approach in nonlinear induction motors," *Int. Trans. Electr. Energy Syst.*, vol. 30, no. 11, pp. 1–19, Nov. 2020.

[17] J. Chiasson, *Modeling and High Performance Control of Electric Machines*. New York, NY, USA: Wiley, 2005.

[18] W. Leonhard, *Control of Electrical Drives*. Berlin, Germany: Springer, 2001.

[19] R. Marino, P. Tomei, and C. M. Verrelli, *Induction Motor Control Design*. London, U.K.: Springer, 2010.

[20] J. Vance, F. Zeidan, and B. Murphy, *Machinery Vibration and Rotordynamics*. Hoboken, NJ, USA: Wiley, 2010.

[21] M. Arias-Montiel, F. Beltrán-Carbajal, and G. Silva-Navarro, "On-line algebraic identification of eccentricity parameters in active rotor-bearing systems," *Int. J. Mech. Sci.*, vol. 85, pp. 152–159, Aug. 2014.

[22] F. Beltran-Carbajal, R. Tapia-Olvera, A. Valderrabano-Gonzalez, H. Yanez-Badillo, J. C. Rosas-Caro, and J. C. Mayo-Maldonado, "Closed-loop online harmonic vibration estimation in DC electric motor systems," *Appl. Math. Model.*, vol. 94, pp. 460–481, Jun. 2021.

[23] Y.-G. Leu and C.-Y. Chen, "B-spline backstepping control with derivative matrix estimation and its applications," *Neurocomputing*, vol. 74, no. 4, pp. 499–508, Jan. 2011.

[24] G. M. Lozito, M. Schmid, S. Conforto, F. R. Fulginei, and D. Bibbo, "A neural network embedded system for real-time estimation of muscle forces," *Proc. Comput. Sci.*, vol. 51, pp. 60–69, Jan. 2015.

[25] C.-F. Hsu and Y.-C. Chen, "Microcontroller-based B-spline neural position control for voice coil motors," *IEEE Trans. Ind. Electron.*, vol. 62, no. 9, pp. 5644–5654, Sep. 2015.

[26] F. Sakr, R. Berta, J. Doyle, H. Younes, A. De Gloria, and F. Bellotti, "Memory efficient binary convolutional neural networks on microcontrollers," in *Proc. IEEE Int. Conf. Edge Comput. Commun. (EDGE)*, Jul. 2022, pp. 169–177.

[27] C. J. B. V. Guimarães and M. A. C. Fernandes, "Real-time neural networks implementation proposal for microcontrollers," *Electronics*, vol. 9, no. 10, p. 1597, Sep. 2020.

[28] C. J. B. V. Guimarães, M. F. Torquato, and M. A. C. Fernandes, "Optimization of MLP neural networks in 8-bit microcontrollers using program memory," in *Proc. Int. Joint Conf. Neural Netw. (IJCNN)*, Jul. 2021, pp. 1–6.

[29] G. Crocioni, D. Pau, J.-M. Delorme, and G. Gruosso, "Li-ion batteries parameter estimation with tiny neural networks embedded on intelligent IoT microcontrollers," *IEEE Access*, vol. 8, pp. 122135–122146, 2020.

[30] T. Salzmann, E. Kaufmann, J. Arrizabalaga, M. Pavone, D. Scaramuzza, and M. Ryll, "Real-time neural MPC: Deep learning model predictive control for quadrotors and agile robotic platforms," *IEEE Robot. Autom. Lett.*, vol. 8, no. 4, pp. 2397–2404, Apr. 2023.

[31] P. Krause, O. Wasynczuk, and S. Sudhoff, *Analysis of Electric Machinery and Drive Systems*. New York, NY, USA: IEEE Press Power Engineering Series, 2002.

[32] F. Beltran-Carbajal, G. Silva-Navarro, and M. Arias-Montiel, "Active unbalance control of rotor systems using on-line algebraic identification methods," *Asian J. Control*, vol. 15, no. 6, pp. 1627–1637, Nov. 2013.

[33] Y. Qin, Z. Wang, K. Yuan, and Y. Zhang, "Comprehensive analysis and optimization of dynamic vibration-absorbing structures for electric vehicles driven by in-wheel motors," *Automot. Innov.*, vol. 2, no. 4, pp. 254–262, Dec. 2019.

[34] F. Beltran-Carbajal, R. Tapia-Olvera, A. Valderrabano-Gonzalez, and I. Lopez-Garcia, "Adaptive neuronal induction motor control with an 84-pulse voltage source converter," *Asian J. Control*, vol. 23, no. 4, pp. 1603–1616, Jul. 2021.

[35] V. Utkin, J. Guldner, and J. Shi, *Sliding Mode Control in Electro-Mechanical Systems*, 2nd ed., Boca Raton, FL, USA: CRC Press, 2009.

[36] H. Yañez-Badillo, F. Beltran-Carbajal, R. Tapia-Olvera, A. Favela-Contreras, C. Sotelo, and D. Sotelo, "Adaptive robust motion control of quadrotor systems using artificial neural networks and particle swarm optimization," *Mathematics*, vol. 9, no. 19, p. 2367, Sep. 2021.

[37] C. J. Harris, C. G. Moore, and M. Brown, *Intelligent Control: Aspects of Fuzzy Logic and Neural Nets*. London, U.K.: World Scientific, 1993.

[38] M. Brown and C. Harris, *Neurofuzzy Adaptive Modelling and Control*. Hertfordshire, U.K.: Prentice-Hall, 1994.

[39] B. Blanchard and W. Fabrycky, *Systems Engineering and Analysis*. London, U.K.: Pearson, 2014.

[40] N. Pathak, T. S. Bhatti, and A. Verma, "New performance indices for the optimization of controller gains of automatic generation control of an interconnected thermal power system," *Sustain. Energy, Grids Netw.*, vol. 9, pp. 27–37, Mar. 2017.

[41] M. Özdemir and D. Öztürk, "Comparative performance analysis of optimal PID parameters tuning based on the optics inspired optimization methods for automatic generation control," *Energies*, vol. 10, no. 12, p. 2134, Dec. 2017.

[42] H. Mujica and G. Espinosa-Pérez, "Control no lineal basado en pasividad de motores de Inducción para alto Desempeño Dinámico," *Revista Iberoamericana de Automática e Informática Ind. RIAI*, vol. 11, no. 1, pp. 32–43, Jan. 2014.

FRANCISCO BELTRAN-CARBAJAL received the B.S. degree in electromechanical engineering from Instituto Tecnológico de Zacatepec, Mexico, in 1993, and the Ph.D. degree in electrical engineering (mechatronics) from Centro de Investigación y de Estudios Avanzados del Instituto Politécnico Nacional (CINVESTAV-IPN), Mexico City, in 2004. He is currently a Titular Professor with the Energy Department, Universidad Autónoma Metropolitana (UAM)–Unidad Azcapotzalco, Mexico City. His main research interests include vibration control, system identification, rotating machinery, mechatronics, and automatic control of energy conversion systems.

HUGO YAÑEZ-BADILLO received the B.S. degree in robotics, the M.S. degree in engineering, and the Ph.D. degree in optomechatronics from Universidad Politécnica de Tulancingo, Hidalgo, Mexico, in 2012, 2015, and 2020, respectively. He is currently a Full Time Professor with the Tecnológico de Estudios Superiores de Tianguistenco (TecNM). Proficient in developing embedded systems for mechatronic applications and signal acquisition and processing, parameter estimation, unmanned aerial systems, mechanical vibrations, electronic power converter control, and intelligent algorithms with applications in robotics systems within the realms of research and industry. His research interests include experimental design and implementation of robust and intelligent control systems.

DANIEL GALVAN-PEREZ received the B.S. degree in robotics engineering and the M.S. degree in automation and control from Universidad Politócnica de Tulancingo, Hidalgo, in 2018 and 2020, respectively, where he is currently pursuing the Ph.D. degree specializing in optomechatronics. His current research interests include the adaptive robust control of manipulator robots' motion for manufacturing applications using laser technology and the adaptive robust control of mobile robots' motion for monitoring and inspection in power systems and smart energy grids.

IVAN RIVAS-CAMBERO (Member, IEEE) received the B.S. degree in electrical engineering from Instituto Tecnológico de Tepic, Tepic, Mexico, in 1998, the M.S. degree in electrical engineering (electrical power systems) from Centro de Investigación y de Estudios Avanzados del Instituto Politécnico Nacional (CINVESTAV-IPN), Unidad Guadalajara, Zapopan, Mexico, in 2002, and the Ph.D. degree in industrial engineering from Universidad Autónoma del Estado de Hidalgo (UAEH), Pachuca, Mexico, in 2012. He is currently a Research Professor with the Research and Postgraduate Department, Universidad Politécnica de Tulancingo (UPT), Tulancingo, Hidalgo, Mexico. His main research interests include the modeling and control of electrical machines and robotic systems.

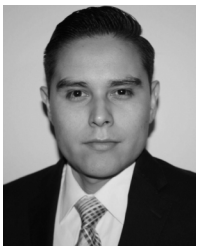

DAVID SOTELO received the B.S. degree in mechatronics engineering from Tecnológico de Monterrey, Monterrey Campus, Monterrey, Mexico, in 2010, the M.S. degree in systems, control, and I&T from Université Joseph Fourier, Grenoble, France, in 2014, and the M.S. degree in automation and control engineering and the Ph.D. degree from Tecnológico de Monterrey, in 2015 and 2019, respectively. Currently, he is ascribed in the Robotics Research Group, Tecnológico de Monterrey, and a member with Mexican National Research System SNI-I. During the Ph.D. degree, he has a several publications. His main research interests include optimal and robust control, process identification, and design of control structures in crude oil distillation columns.

CARLOS SOTELO received the B.S. degree in mechatronics engineering from Tecnológico de Monterrey, Monterrey Campus, Monterrey, Mexico, in 2010, the M.S. degree in systems, control, and I&T from Université Joseph Fourier, Grenoble, France, in 2014, and the M.S. degree in automation and control engineering and the Ph.D. degree from Tecnológico de Monterrey, in 2015 and 2019, respectively. He is currently ascribed with the Robotics Research Group, Tecnológico de Monterrey, and a member with Mexican National Research System SNI-I. During the Ph.D. degree, he has a several publications. His main research interests include nonlinear control, mechatronics, parametric identification, and predictive control of refinery processes.